Geophys. J. Int. (1990) **103,** 509–531

The ocean–continent boundary off the western continental margin of Iberia—I. Crustal structure at 40°30′N

R. B. Whitmarsh,[1] P. R. Miles[1] and A. Mauffret[2]

[1] *Institute of Oceanographic Sciences Deacon Laboratory, Wormley, Godalming, Surrey* GU8 5UB, *UK*
[2] *Département de Géologie Dynamique, Université Pierre et Marie Curie, 4 Place Jussieu, 75230 Paris Cedex 05, France*

Accepted 1990 June 20. Received 1990 April 30; in original form 1989 November 16

SUMMARY

The western continental margin of the Iberian peninsula has the characteristics of a rifted non-volcanic margin with half-graben and tilted fault blocks seen in several places. The ocean–continent boundary (OCB) is therefore expected to be where thinned continental crust and oceanic crust are juxtaposed, as at many similar margins worldwide. It is particularly useful to locate the OCB off western Iberia in order to constrain the pre-rift fit of North America to Iberia and, by implication, the shape of the proto-Bay of Biscay. The fit is only marginally constrained by sea-floor spreading magnetic anomalies because anomaly 34 is believed to be far to the west of the OCB and it is even possible that all older oceanic crust was created during the Cretaceous constant polarity interval. The best way to distinguish oceanic crust from thinned continental crust appears to be the crustal seismic velocity structure. Therefore in 1986 a series of seismic refraction lines was shot parallel to, and normal to, the continental margin. These lines enabled us to bracket the location of the OCB. A further constraint on the location was obtained by modelling an east–west magnetic profile which included the enigmatic J-anomaly. This anomaly can be explained as either just pre-anomaly M0 or as part of the Cretaceous constant polarity interval, depending on whether spreading began about 127 or after 118 Myr ago, respectively. The evidence favours the former explanation. Lastly the depth to acoustic basement was contoured from a compilation of seismic reflection profiles. This indicated a new fracture zone at 41°15′N which offsets the OCB. A few key reflection profiles also suggest that the OCB can be identified by an abrupt landward step-down in acoustic basement. We conclude that the OCB in the eastern Iberia Abyssal Plain lies between 12°10′ and 12°30′W and has a trend just east of north. This westerly location is consistent with recent estimates of the location of the OCB off the Grand Banks but brings into question the proposed location at about 11°W of the OCB in the Tagus Abyssal Plain.

Key words: continental margin, Iberia, North Atlantic, ocean–continent boundary, seismic structure.

INTRODUCTION

The western continental margin of the Iberian peninsula extends from the latitude of Cape Finisterre at about 43°N to the latitude of Cape Saint Vincent at about 37°N (Fig. 1). The margin has the characteristics of a non-volcanic rifted margin with a narrow shelf. The earliest multichannel reflection profiles recognized fault-bounded horst and graben structures beneath the northern half of the margin (Montadert *et al.* 1974) but the typical combination of half-graben and tilted blocks was only clearly recognized following site surveys for scientific drilling west of Galicia Bank (Groupe Galice 1979; Sibuet *et al.* 1987; Mauffret & Montadert 1987). Further south, adjacent to the Tagus Abyssal Plain, block faulting has also been recognized on multichannel profiles across the margin by Mougenot *et al.* (1979) and by Mauffret *et al.* (1990).

The sea-floor spreading magnetic anomaly pattern west of Iberia (Verhoef *et al.* 1986) is unhelpful in precisely constraining either the age of break-up of the margin or the

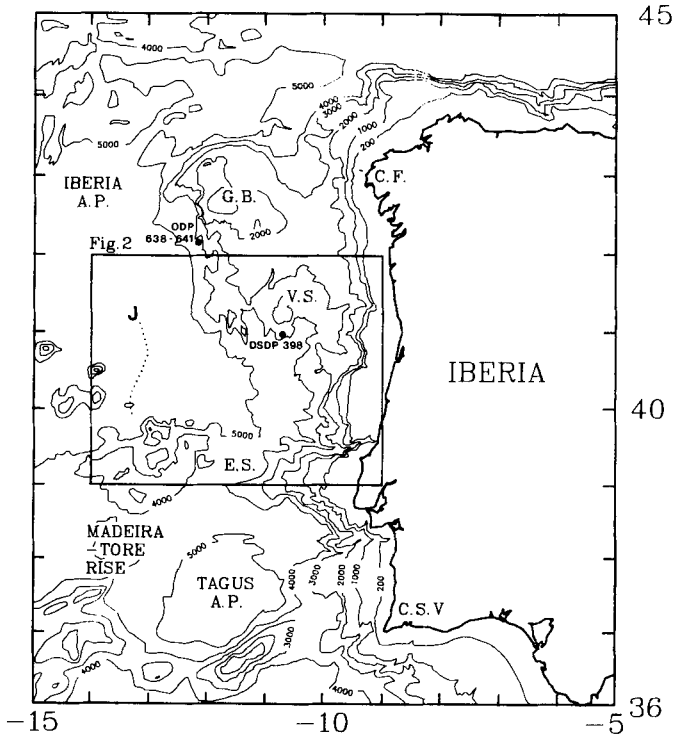

Figure 1. Generalized bathymetry of the western continental margin of Iberia (contours in metres) G.B. = Galicia Bank; V.S. = Vigo Seamount; A.P. = abyssal plain; C.F. = Cape Finisterre; C.S.V. = Cape Saint Vincent; E.S. = Estremadure Spur; J = J-anomaly. Dots denote DSDP/ODP drill sites.

location of the ocean–continent boundary (OCB). Although the polarity reversal at anomaly 34 is clearly seen between 37°N, 19°30'W and 44°N, 17°W east of this there is a region over 3000 m deep and up to 650 km wide, which includes oceanic crust formed in the Cretaceous constant polarity interval (MQZ), within which no continuous linear anomaly of comparable length can be discerned. An enigmatic generally north–south strong positive anomaly, originally labelled J by Pitman & Talwani (1972) and which has been identified as anomaly M0 (Srivastava *et al.* 1988), reaches as far north as about 41°N where it abruptly ends. This anomaly appears to transgress the NNE-trending Madeira–Tore Rise (Verhoef *et al.* 1986). We shall discuss its origin later. Srivastava, Verhoef & MacNab (1988) have also found an anomaly K within the Cretaceous MQZ which they believe to represent an isochron.

The tectonic history of the west Iberia margin includes several distinct phases of activity (Masson & Miles 1986). Briefly, pre-drift rifting occurred over a protracted period of Mesozoic time. The break-up unconformity was recognized to lie between Late Aptian and early Albian in drillholes both west of Galicia Bank (Boillot *et al.* 1987) and at Site 398 adjacent to Vigo Seamount (Sibuet *et al.* 1979). This predates the break-up unconformity drilled off Goban Spur (Masson, Montadert & Scrutton 1984) by at least 6 Ma [based on the magnetobiostratigraphic time-scale of Kent & Gradstein (1986) which is used throughout this paper]. No oceanic drillholes exist south of Vigo Seamount on this margin. During the Eocene Pyrenean orogeny the region underwent compression with a northerly component. This reactivated some of the rift faults thereby uplifting individual basement blocks by as much as 2500 m to produce features such as Galicia Bank and Vasco da Gama, Porto and Vigo seamounts (Mougenot *et al.* 1984). Further, but less intense, compression occurred during the Miocene Betic orogeny (op. cit.), primarily south of Galicia Bank (Mauffret *et al.* 1990).

The above discussion highlights the difficulties in fitting Iberia to the conjugate Canadian margin, which lies on the southeast side of the Grand Banks. The problem is exacerbated by the fact that Galicia Bank and Flemish Cap (northeast part of the Grand Banks) both extend some 200 km oceanward from their respective continents. The overlap sometimes permitted between the two features has given rise to a great variety of reconstructions (e.g. Masson & Miles 1984; Olivet *et al.* 1984; Klitgord & Schouten 1986; Srivastava & Tapscott 1986; Srivastava *et al.* 1988).

Off the southern part of the margin the problem is compounded by the presence of the Madeira–Tore Rise, which is likely to be of volcanic origin, and by the present-day diffuse seismicity east of the Rise which results from relative motion between the African and Eurasian plates.

An important constraint, which is missing from all reconstructions, is the precise position of the ocean–continent boundary off Iberia. For example such knowledge might substantiate, limit, or even eliminate, claims that the Tagus Abyssal Plain is underlain by oceanic crust (Klitgord & Schouten 1986; Mauffret *et al.* 1990). At present even the most precise and quantitatively best-constrained fits of Masson & Miles (1984) and Srivastava *et al.* (1988) leave a gap of several hundred kilometres where the eastern Iberia and Tagus Abyssal Plains now lie. Therefore in 1986 a series of seismic refraction lines were shot in the eastern Iberia Abyssal Plain to determine the location of the ocean–continent boundary. The results are presented here. Additional refraction data acquired in the Tagus Abyssal Plain also on Discovery Cruise 161 will be published later.

SEISMIC REFRACTION LINES

Four refraction lines, up to 105 km long (Fig. 2), were shot with digital ocean-bottom seismographs (Kirk, Langford & Whitmarsh 1982; Peal & Kirk 1983). An array of four 16-litre airguns was fired out to about 30 km and at greater ranges shots of 25, 50 or 125 kg of ICI Opencast Gelignite Bulkpack, initiated by slow-burning fuse, were used. Shot-to-receiver ranges were calculated from water-wave traveltimes and from a soundspeed structure deduced from a nearby XBT cast down to 570 m and from historical water-bottle casts at greater depths.

Three of the lines (Lines 1, 2, 3) were located parallel to the expected regional strike to provide an evenly spaced sampling of crustal thickness from the foot of the continental slope to just east of the large positive J magnetic anomaly which terminates at about 41°N, 13°W. A strike-normal line (Line 4) was fired in the vicinity of, and across, the westmost parallel line with the expectation that, since it crossed anomaly J, it would transect the ocean–continent boundary thereby enabling the OCB to be located quite precisely.

It is evident from a study of the record sections and

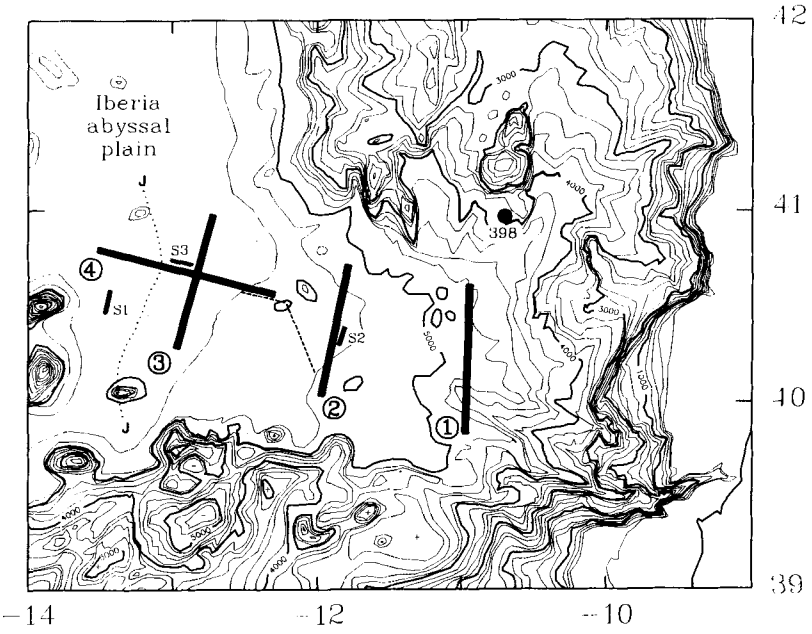

Figure 2. Bathymetry in the vicinity of the seismic refraction lines (1, 2, 3 and 4). S1, S2 and S3 denote disposable sonobuoy lines. 398 denotes DSDP Site 398. Contour interval is 200 m. J = J-anomaly. Dashed line is location of seismic reflection profile in Fig. 19.

associated reflection profiles that variations in the depth to acoustic basement have perturbed traveltimes significantly. Thus ray tracing was used to model travel time observations. This was done with a computer program based on a 2-D technique which uses Maslov transforms (Chapman & Drummond 1982). The acoustic basement and major intrasediment reflectors were digitized from reflection time-sections. Sediment velocities based on the results of three disposable sonobuoy lines (Table 1, Fig. 2) were used to transform each digitised time-section to a depth-section. Ray tracing then proceeded by progressively adding layers to the bases of a 2-D model in such a way as to satisfy the observed traveltimes. The bases of such layers frequently could be made to follow approximately the shape of the acoustic basement. Deeper layers tended to be more planar.

A principal objective of the work was to discover the extent of thinned continental crust and, if possible, the location of the ocean–continent transition. The best seismic method to differentiate between oceanic and thinned continental crust appears to be the nature of the lower crust (Whitmarsh, Avedik & Saunders 1986). Oceanic crust typically contains a 6.7–7.1 km s^{-1} layer 3 with a weak gradient whereas thinned continental crust typically exhibits lower velocities than this with a stronger gradient. Therefore, in order to obtain the best estimate of the structure of the lower crust the optimum traveltime (ray-trace) model for each line was perturbed out to about 30 km range, where usually closely spaced airgun traces also provided tight control, to obtain a satisfactory fit of synthetic seismograins with the observations (Chapman & Drummond 1982). These seismograms include the effects of both vertical and horizontal velocity variations within the ray-tracing models. The resulting velocity profiles therefore are strictly valid only within about 30 km of the relevant DOBS.

LINE 1

This north–south line was located in about 4800 m water depth over a reflection profile obtained on an earlier cruise (Fig. 2). A digital ocean-bottom seismograph (DOBS) was deployed at each end of the line, the southern one lying just south of the channel and levee running west from the Nazaré canyon. Some 2.4–3.7 km of sediment overlie a generally smooth and almost level acoustic basement. Due to technical problems the northern DOBS recorded only six explosion shots.

A composite airgun and explosion record-section for DOBS 2 appears in Fig. 3. Particularly strong first arrivals are evident to 25 km; thereafter the amplitude is fairly constant but drops quite substantially in the range to 40–60 km. A clear 4.9 km s^{-1} second arrival appears

Table 1. Sonobuoy interval velocities.

Sonobuoy	Position	Depth (m)	V1 (km/s)	H1 (m)	V2 (km/s)	H2 (m)	V3 (km/s)	H3 (m)	V4 (km/s)	H4 (m)
1	40°27.2'N 13°29.7'W	5354	1.84	420	2.26	575	2.70	310	-	-
2	40°22.0'N 11°51.9'W	5231	1.85	798	2.39	670	2.90	500	3.40	710
3	40°37.1'N 12°51.7'W	5354	1.86	575	2.30	700	2.70	410	3.44	850

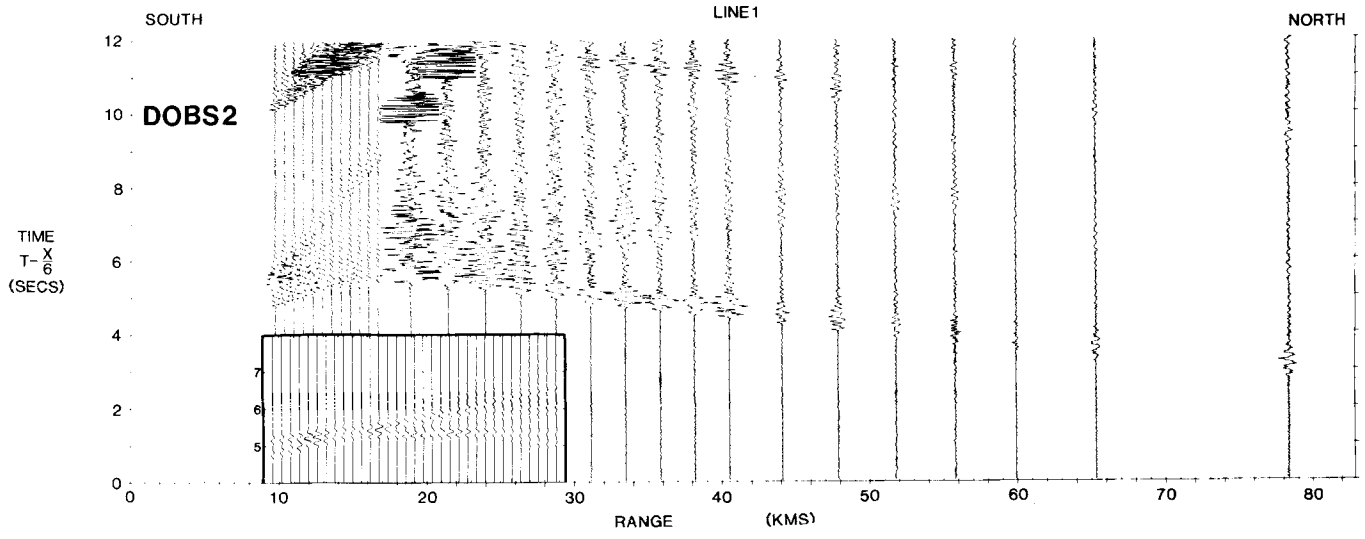

Figure 3. Record section for DOBS 2 at the south end of Line 1. The section is composed of every other airgun trace (LP 12 Hz) and all explosion traces (unfiltered). Trace amplitude was scaled by distance. The relative amplitude of gun and explosion traces is arbitrary. Inset, synthetic seismograms calculated by the WKBJ method and Maslov ray tracing.

between 30 and 40 km. The model derived from ray tracing and the associated travel time plot are shown in Fig. 4. The principal features of the model are the 0.5° southward dip of the Moho and the thickened crust under the basement high at 65 km. The extreme north end of the model is not well constrained due to difficulty in identifying the acoustic basement on the reflection profile. It is not possible to get agreement within 0.15 s between the arrival times of apparent mantle arrivals at DOBS 1 and the longest range shots recorded by DOBS 2; a mid-crust refractor near DOBS 1 might be one solution.

The synthetic seismogram modelling attempted to reproduce the following features of the first arrivals on the DOBS record-section which are relevant to the crustal structure; weak first arrivals at 14 km, strong explosion arrivals in the range 16–24 km and weaker arrivals beyond 26 km. It was not possible to clearly correlate second arrivals from trace to trace beyond 18 km on the airgun record-section because of low gun pressure. The former features were modelled by the introduction of a relatively steep gradient in the upper non-sedimentary crust and by a transitional Moho (Fig. 12).

LINE 2

Line 2 lay 70–80 km west of Line 1 and 40 km east of the east end of Line 4 (Fig. 2). A DOBS was deployed at each end of the line. A nearly coincident seismic reflection profile detected a slightly southward dipping acoustic basement with maximum relief of 1 s. Unfortunately the profile ended about 13 km short of the southern DOBS.

Airgun shots and explosions were recorded by both DOBS so that the record-sections are complete (Fig. 5). The record-section of DOBS 1 at the north end of the line has clear first arrivals, except between 14 and 29 km where they are often weak. Very little energy is apparent between the first arrivals and their sea-surface reflected multiples. A strong 3.0 km s^{-1} shear-wave second arrival is also seen out to about 24 km. The upper mantle arrivals have an apparent velocity of only 7.7 km s^{-1}.

The DOBS 2 record-section is rather different. The airgun first arrivals are even clearer than for DOBS 1. On almost all explosive traces, beginning about 2 s after the first arrival onset, a strong 4 Hz oscillatory ringing can be seen which is unlikely to be of instrumental origin. At ranges less than 30 km several groups of 3.3 km s^{-1} second arrivals probably indicate multiple generation, within the upper sedimentary layer, from energy returned from the lowermost sediment. Finally upper mantle arrivals have an apparent velocity of about 8.4 km s^{-1} which, compared with DOBS 1, indicates that there is a significant southward component of a dip of the Moho along the line.

Traveltime modelling was restricted by the lack of a reflection profile close to DOBS 2 and by uncertainty in the location of acoustic basement near DOBS 1. The latter problem is likely to be the cause of poor traveltime fits in the range 70–80 km from DOBS 2 (Fig. 6). The result of this modelling was to suggest that the Moho has a 2.5° southward component of dip with the lower crust thickening in the same direction.

The airgun part of the DOBS 2 record-section was chosen for amplitude modelling because it had a significantly greater crust/mantle cross-over distance (i.e. thicker crust) than for DOBS 1 and therefore promised to provide much better depth resolution within the crust. Significant features on the observed record-section include the relatively weak first arrivals in the range 24–30 km and the strong sediment first arrivals out to 15 km which then persist as second arrivals to about 20 km. The set of best fitting synthetic seismograms can be seen in Fig. 5 with a representative velocity/depth profile in Fig. 12.

LINE 3

This NNE-trending profile was situated about 30 km east of, and parallel to, the large positive J magnetic anomaly in the

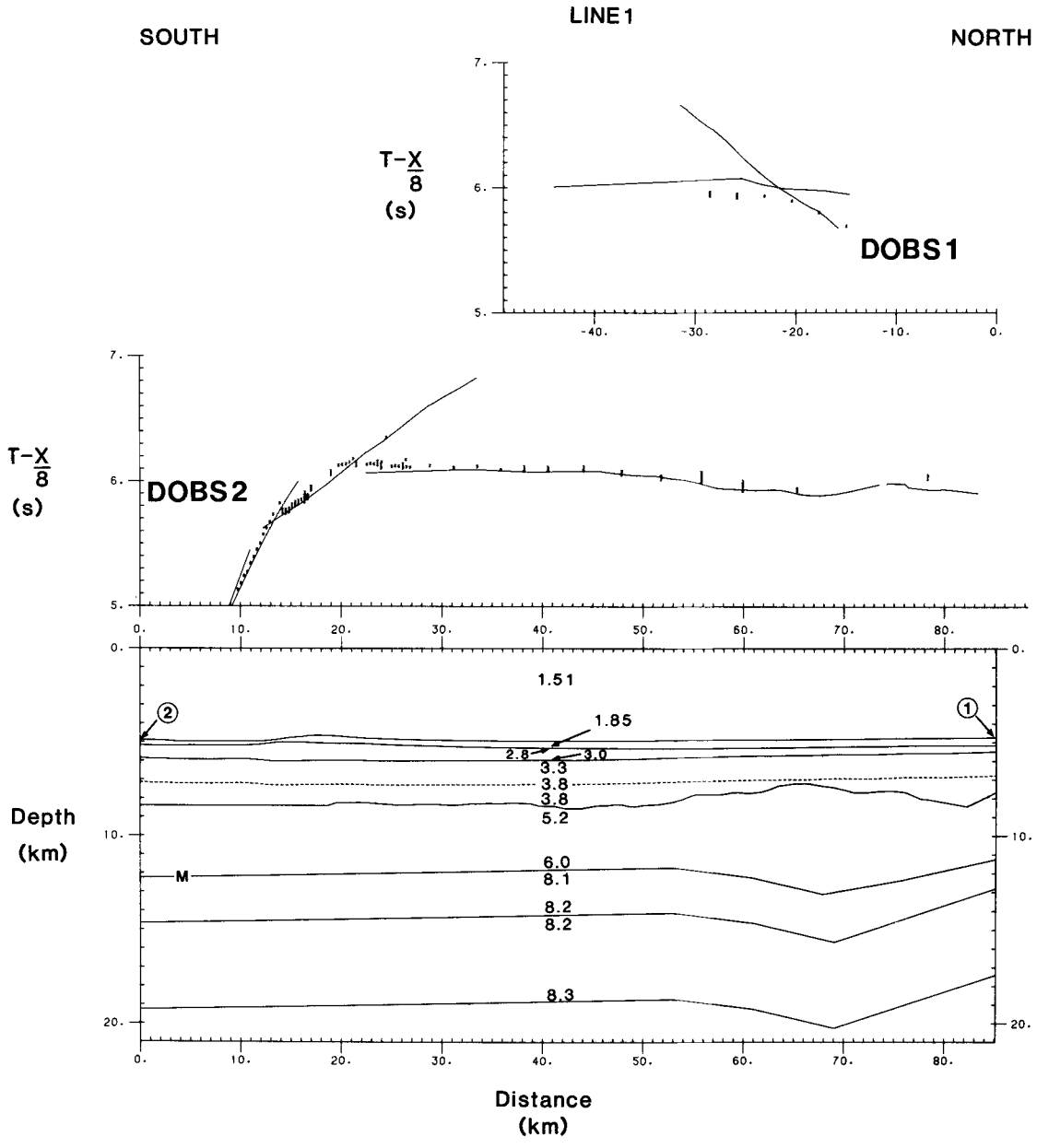

Figure 4. Results of the ray-tracing used to match the observed Line 1 traveltimes (black bars). The lengths of the bars denote the precision of the picked times. Continuous lines were calculated by ray tracing. The corresponding velocity–depth model appears below (velocities in km s^{-1}). DOBS locations are indicated by circled number. M = Moho.

eastern Iberia Abyssal Plain (Fig. 2). A DOBS was deployed at each end of the line. A reflection profile along the line showed sediment mostly 1–2.4 km thick and generally thickening southwards.

Both airgun shots and explosions were recorded by DOBS 2 (south end) whereas only explosions were recorded by DOBS 4 (Fig. 7). DOBS 2 has clear 3.4 km s^{-1} first arrivals from the lower sedimentary section which are intersected by a second set of arrivals at 14 km. Second arrivals with an apparent velocity 5.6 km s^{-1} can be seen between 16 and 20 km. Lastly strong Moho reflections are observed from 29 to 36 km. Less detail is seen on the DOBS 4 record-section where most first arrivals have an apparent velocity of 7.5 km s^{-1}.

In modelling the DOBS 2 traveltimes a layer had to be inserted between the sediments and the 5.1 km s^{-1} refractor. A velocity of 4.0 km s^{-1} was assumed. If the first DOBS 4 arrival at 12 km is assumed to be from the 5.1 km s^{-1} refractor then the 4.0 km s^{-1} layer must be thinner there; a taper of the 4.0 km s^{-1} layer was assumed (Fig. 8). The form of the top of the lower crustal layer (7.55–7.7 km s^{-1}) is well determined by reversed arrivals. Mantle arrivals are seen only by DOBS 2 even though there are clear first arrivals at DOBS 4 out to 76 km. One explanation for the absence of mantle arrivals at DOBS 4 could be that they are deflected downwards by a relatively steep northward dipping Moho north of 68 km which would be qualitatively consistent with isostatic compensation of the

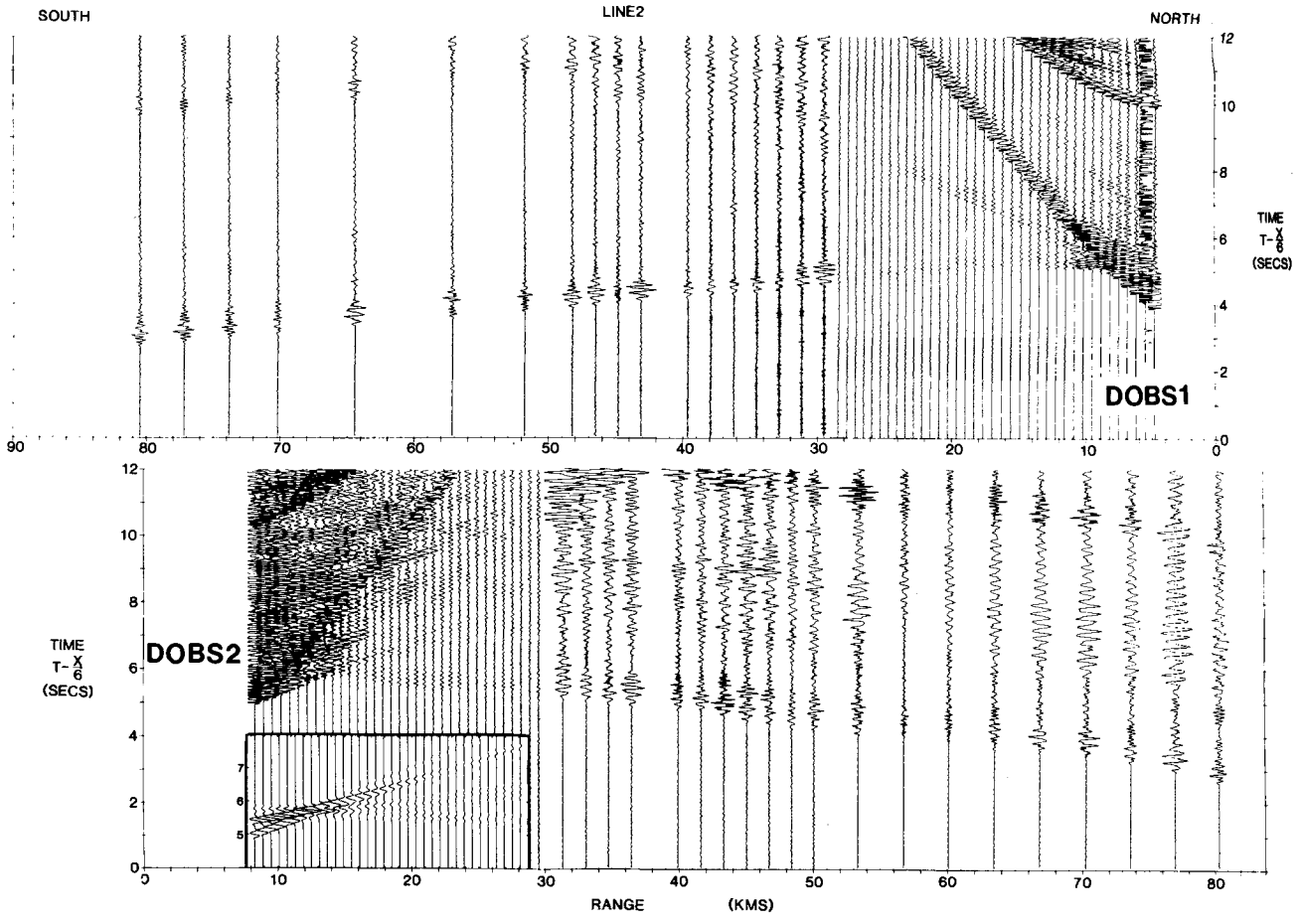

Figure 5. Record sections for DOBS 1 and 2 at Line 2. Both sections are composed of every other airgun traces and all explosion traces. Inset, synthetic seismograms. See Fig. 3 for further explanation.

relatively shallow basement north of 60 km. The best ray-trace model and corresponding traveltime curves are shown in Fig. 8.

Synthetic seismograms were used to model the DOBS 2 airgun record-section, since this possesses details, visible in the closely spaced traces, which are relevant to the crustal structure. Thus modelling attempted to reproduce not only the varying amplitude of the first arrivals but also the second arrivals seen from 12 to 18 km and 17 to 20 km as well as the strong Moho reflection. The greatest difficulty was experienced in obtaining sufficiently strong and late Moho reflections. The closest approach to the observed traces came from invoking a Moho transition of alternating crust and mantle velocity layers whereby successful multiples within the layers arrived in phase at the OBS. The resulting synthetic record-section appears in Fig. 7 with a typical velocity/depth structure in Fig. 12.

LINE 4

Line 4 was shot perpendicular to Line 3 and crossed the large positive J magnetic anomaly at its western end (Fig. 2). As well as the DOBS at each end of the line a third DOBS was deployed about 40 km from the east end to try to define better the expected lateral inhomogeneities in the crust. The line lay entirely within the Iberia Abyssal Plain. A reflection profile along its length shows an irregular basement with up to 1.5 s of basement relief and sediment thicknesses from 1.0 to 2.6 km. The shallowest basement lies just west of the axis of the J magnetic anomaly.

The record-sections appear in Fig. 9. Excellent crustal arrivals are seen at the westernmost DOBS (DOBS 1) out to the region of the mantle critical point. Beyond 40 km however the mantle arrivals become weaker and are too weak to be discerned beyond 60 km (even for the 125 kg shot at 64 km). Good crustal arrivals are also seen at the easternmost DOBS (DOBS 4) but here clear mantle arrivals persist to 106 km. Due to a shipboard technical problem the airgun shots that were recorded by the central DOBS (DOBS 2) were at ranges where the explosions provided better data. Unlike the arrivals from shots more than 60 km east of DOBS 1 the arrivals out to 60 km west of DOBS 2 are quite clear suggesting a dramatic change in structure or attenuation in the lower crust or mantle beyond or in the vicinity of DOBS 2. The shots to the east of DOBS 2 provide good data out to the most distant shot at 36 km.

Modelling the traveltimes was complex because of the high basement relief and the several constraints imposed by the various reversed sections of the model. DOBS 4 gives clear evidence from the 12 to 29 km first arrivals for a lower crust with velocities in the range 6.4–6.7 km s^{-1}. 3.3 km s^{-1} arrivals at shorter ranges, not easily seen in Fig. 9 because

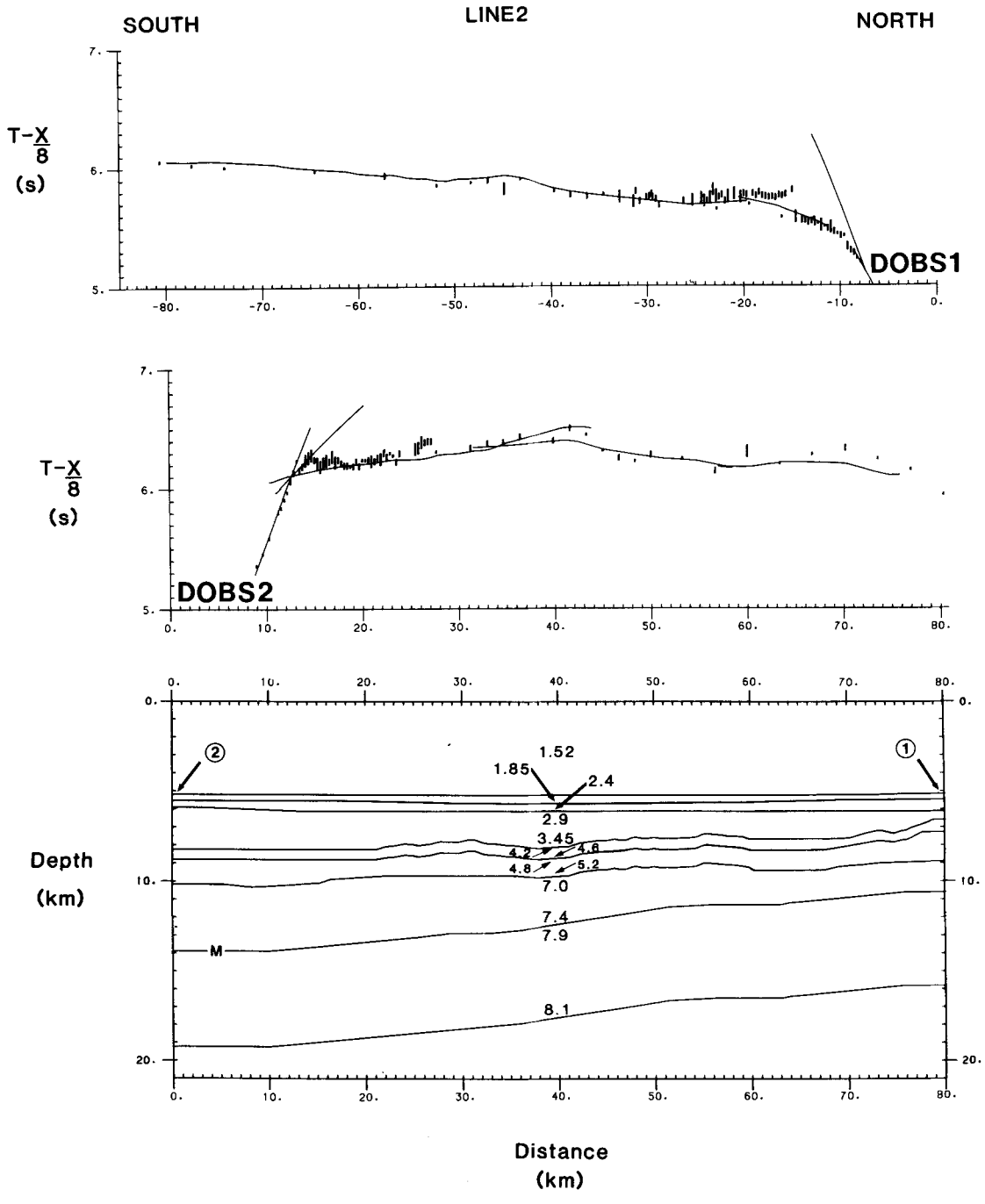

Figure 6. Results of the ray tracing used to match the observed Line 2 traveltimes (black bars). See Fig. 4 for further explanation.

alternate traces have been omitted, clearly come from the lower sediments. It is particularly striking how the substantial traveltime variations of the DOBS 4 mantle arrivals can be fitted by ray tracing (Fig. 10).

DOBS 1 indicates a very different crustal structure from DOBS 4. Firstly arrivals in the range 8–12 km and 12–26 km indicate velocities of about 5.4 and 7.1 km s^{-1} respectively. It was necessary to insert a layer between the base of the sediments and the 5.4 km s^{-1} layer and, as at Line 3, a velocity of 4.0 km s^{-1} was assumed for this layer. A similar problem existed at DOBS 4. Consequently it was assumed that both upper crustal layers extended the whole length of Line 4. To fit the lower crust arrival times it was necessary to introduce a westward thickening taper to the upper crustal layers. In doing so the shape of the base of these layers was made to closely follow the form of the acoustic basement (Fig. 10).

The arrivals at DOBS 2 could be reconciled with the constraints imposed by DOBS 1 and 4 particularly for the lower crust and mantle. The location of DOBS 2 in between two basement ridges gives rise to rather complex traveltime curves for upper crust arrivals in the range 0–20 km. First arrivals east of DOBS 2 clearly indicate a 6.4 km s^{-1} layer. However no mantle first arrivals are clearly seen out to

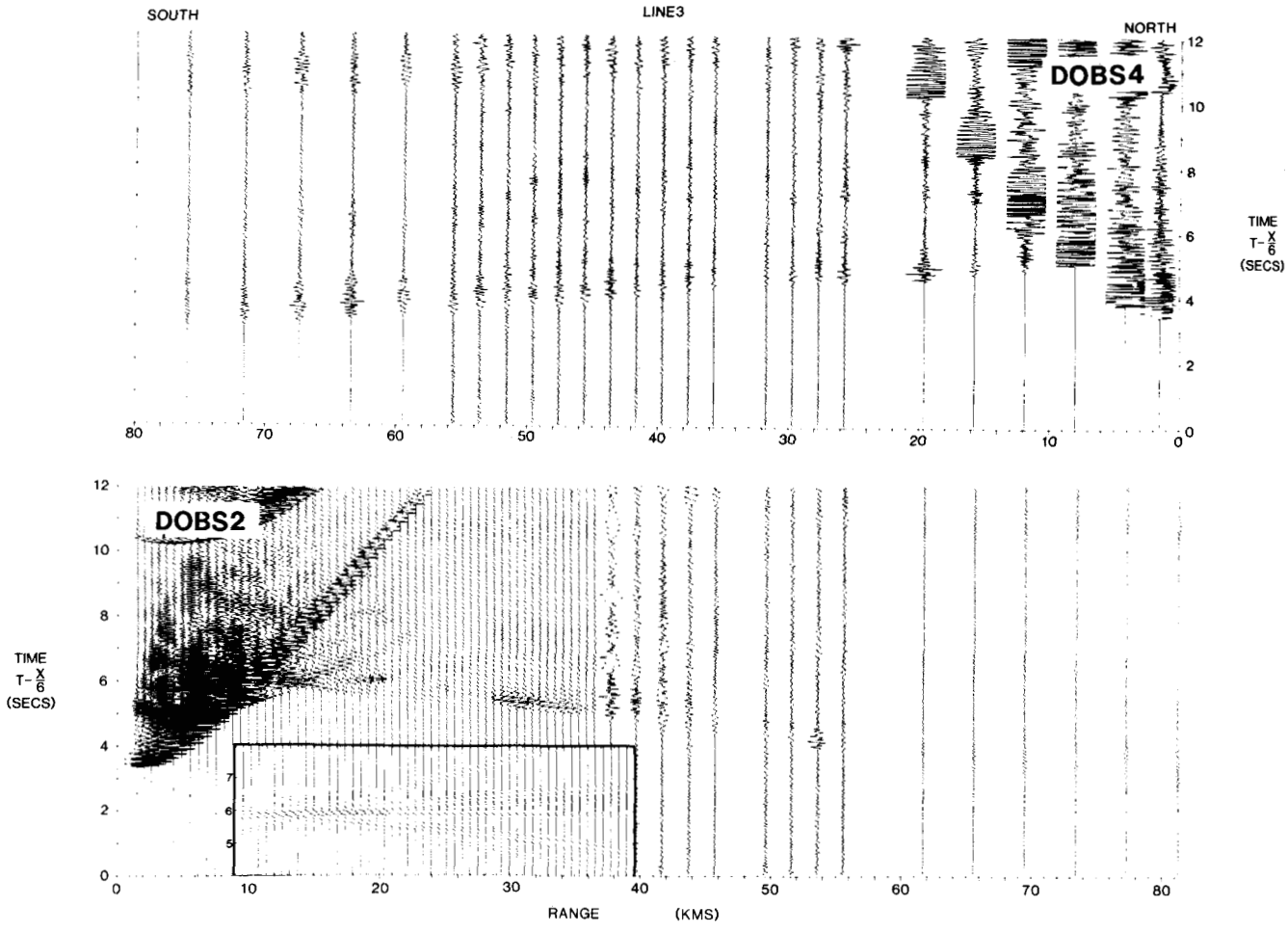

Figure 7. Record sections for DOBS 2 and 4 at Line 3. The DOBS 2 section is composed of every other airgun trace out to 36 km (LP 15 Hz) and all explosion traces (unfiltered); DOBS 4 recorded only explosions. Inset, synthetic seismograms. See Fig. 3 for further explanation.

36 km which again may be evidence for poor mantle or lower crust transmission immediately east of DOBS 2. To the west the evidence for 7.3/7.6 km s^{-1} in the lower crust is not strong; a thinner slower layer is possible but the chosen velocities fit better with Line 3 which intersects Line 4 in this region about 52 km from DOBS 4.

Finally the crustal structure at each end of Line 4, where closely spaced airgun traces were recorded, was checked using synthetic seismograms (Fig. 9). This confirmed in particular the striking differences in lower crustal structure between the two ends of the profile.

On the DOBS 1 record-section, besides the relative amplitudes of the first arrivals, a strong second arrival seen between 9.5 and 12.5 km was modelled. The high-frequency aspect of the first arrivals beyond 14 km was not modelled; this is not seen elsewhere along Line 4 and is probably due to a local effect in the vicinity of DOBS 1.

On the DOBS 4 record-section the modelled features were the first arrival amplitudes and the strong Moho reflections seen between 17 and 19 km. It was not possible to reproduce the strong first arrivals between 23 and 25 km. These arrivals may have been focused by a basement depression which was not well imaged on the seismic reflection profile.

Representative velocity/depth profiles are shown in Fig. 11.

DISCUSSION

Representative velocity/depth profiles, extracted from the models constrained by synthetic seismograms, appear in Fig. 12 to illustrate the changing crustal structure from Line 1 oceanward. Each profile has been picked at a point in the model which is roughly at the centre of the modelled seismograms.

Beneath the gently westward-sloping sea-floor there is a clear wedge of sediment, bounded below by the acoustic basement, which thins westward from about 3.5 km to about 2 km or less. There is indirect evidence (from synthetic seismograms) that the velocity in the lower part of this wedge reaches 4.1 km s^{-1} beneath Line 1; there is direct evidence of 3.3 and 3.4 km s^{-1} velocities beneath Lines 3 and 4. Since, as will be shown later, we believe Lines 3 and 4 to be on oceanic crust it is likely that most, if not all, of the sedimentary section overlying basement is of post-rift origin.

The velocity profiles between the basement and the Moho present, at first sight, a perplexing variety of forms. We

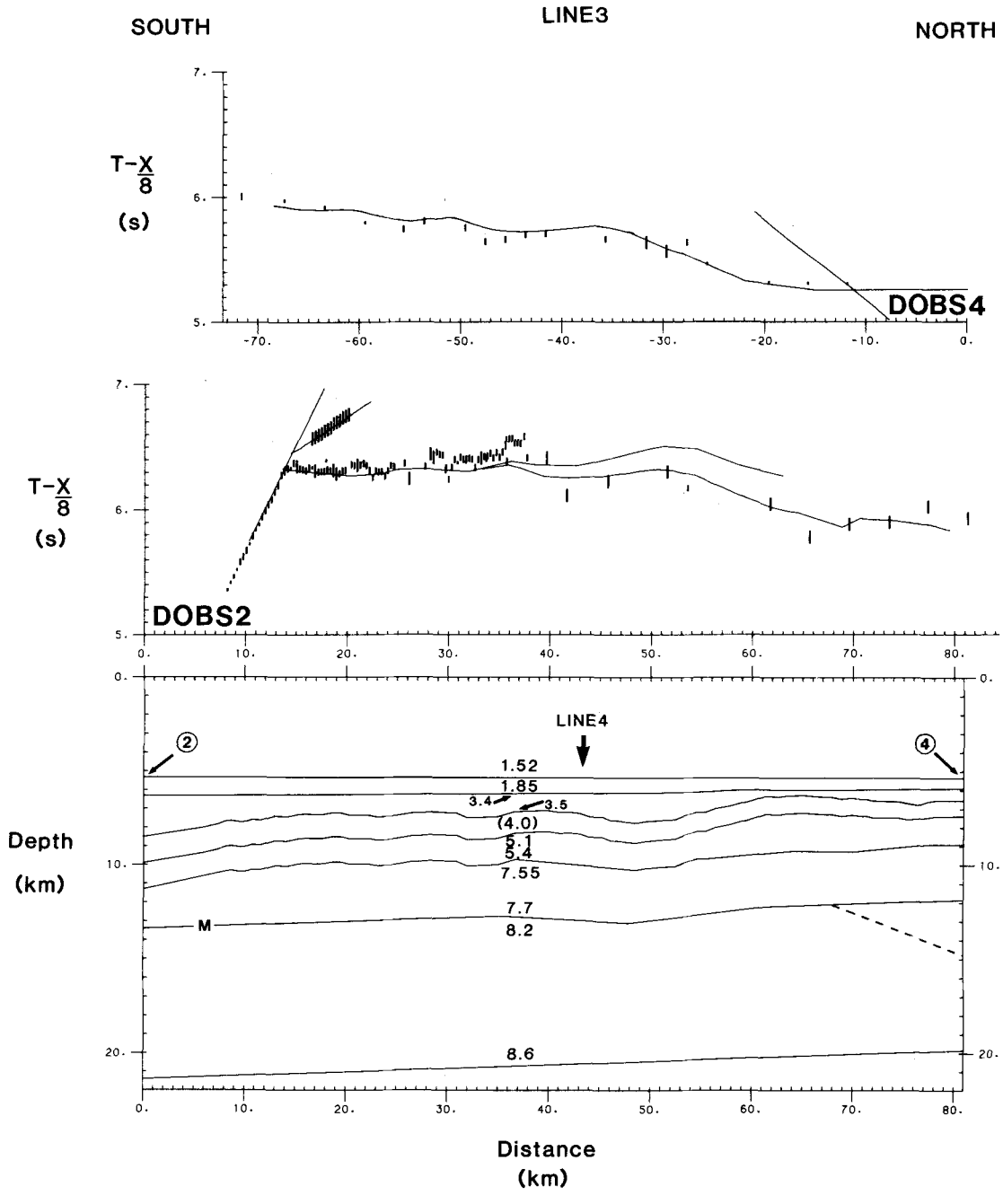

Figure 8. Results of the ray tracing used to match the observed Line 3 traveltimes (black bars). The vertical arrow marks the intersection with Line 4. The dashed line is a schematic indication of the type of Moho feature which can mask mantle arrivals at DOBS 4 (see text). Assumed velocity in parentheses. See Fig. 4 for further explanation.

chose initially to attribute a particular origin to each crustal section purely on the basis of the seismic velocities, and therefore needed to establish the typical features of Iberian continental crust as well as of North Atlantic oceanic crust.

It is well known that at non-volcanic rifted margins the continental crust may have been thinned to less than 1/5 of its original thickness. The extent to which original features of the unthinned crust are preserved is not known but a clear starting point is the nature of the crust under western Iberia. Geologically, western Iberia consists of the Hercynian Iberian Massif which is overlain by Mesozoic sedimentary basins along the coast between 38° and 41°N. A reversed profile along the coast near Nazare (Line M, Fig. 13) indicated a linear velocity gradient within the Mesozoic and, in some places, Tertiary sediments with velocities increasing downwards from 4.0 to 4.6 km s^{-1} at the surface. The base of the Mesozoic sediments is not clear; there is probably a gradual transition to Palaeozoic sediments and then crystalline basement with a velocity of 6.5 km s^{-1} (Moreira *et al.* 1982). A second NW–SE line through Peniche (Line MV, Fig. 13) found that an average velocity of 4.5–5.0 km s^{-1} was required for the Mesozoic sediments

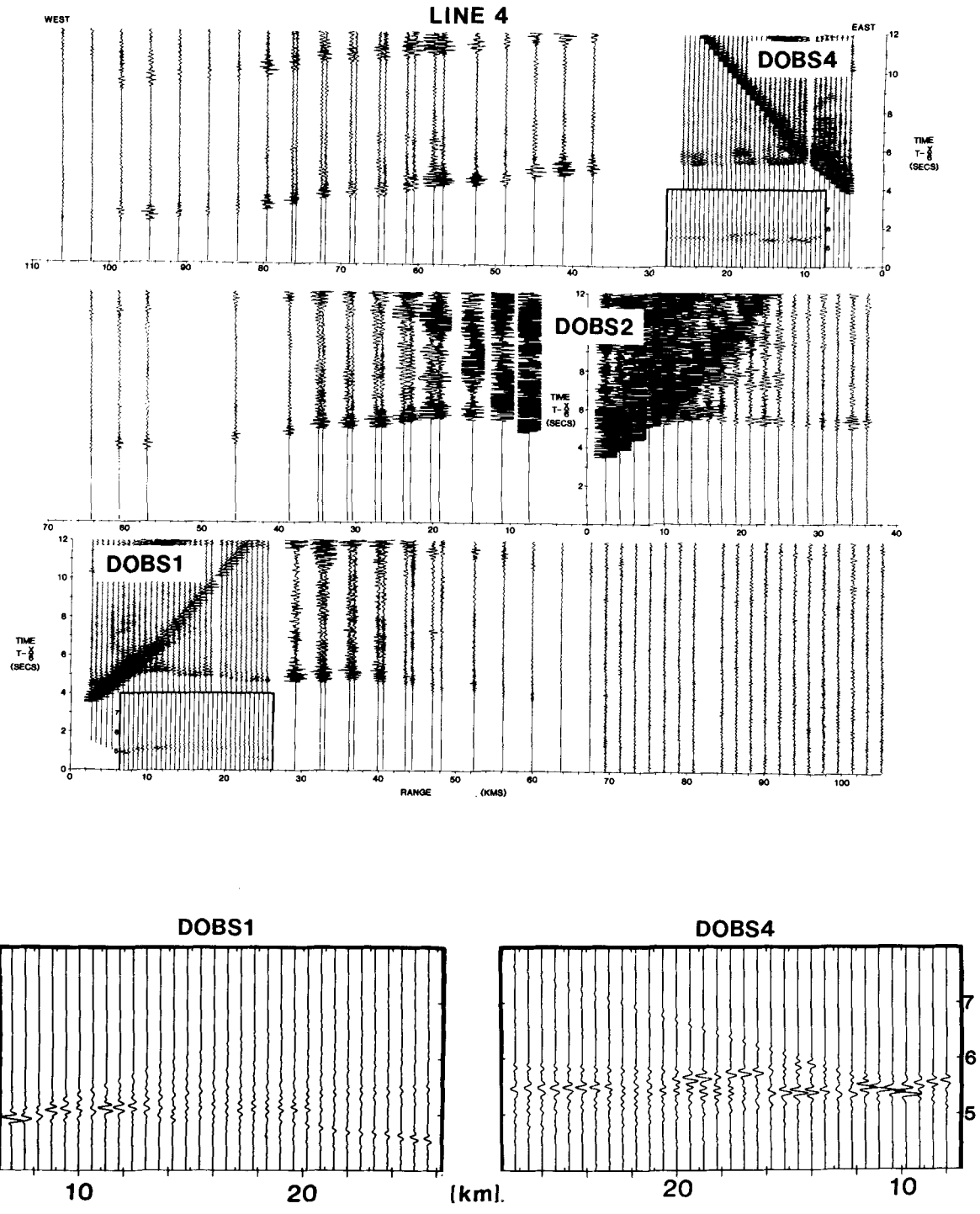

Figure 9. Record sections for DOBS 1, 2 and 4 at Line 4. The DOBS 1 and 4 sections are composed of every other airgun trace and all explosion traces; DOBS 2 section contains explosion traces only. Insets, synthetic seismograms which are enlarged at the bottom of the diagram. See Fig. 3 for further explanation.

up to 5 km thick for *Pg* traveltimes to be consistent with deep borehole data (Mendes Victor, Hirn & Veinante 1980). Banda *et al.* (1981) report an unreversed E–W line 270 km long west of Toledo (Line B, Fig. 13). The basement rocks have a velocity of 6.1 km s^{-1}. The lower crustal velocity does not exceed 6.9 km s^{-1}. There is a transitional Moho, at least 1.5 km thick, at about 31 km depth. In the Galicia province of NW Spain Cordoba, Banda & Ansorge (1987) reported a 250 km long NE–SW coast-to-coast reversed profile (Line C, Fig. 13). A similar structure was obtained, i.e. 6.1–6.2 km s^{-1} upper crust over 6.7–6.9 km s^{-1} lower crust, but a sharp Moho boundary was favoured. In places the surface velocity of the granite was as low as 5.1 km s^{-1}. In summary therefore in western Iberia

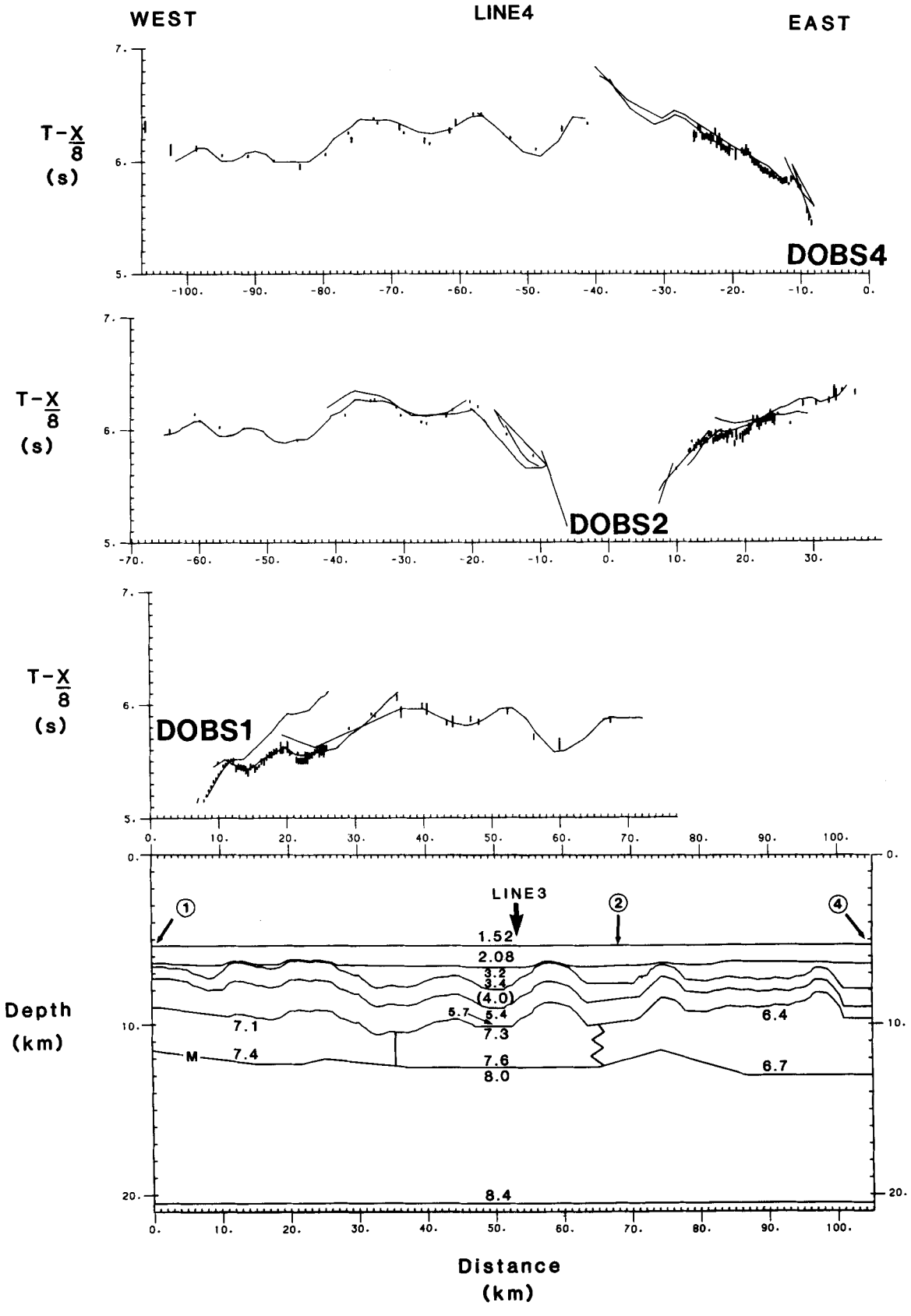

Figure 10. Results of the ray tracing used to match the observed Line 4 traveltimes (black bars). The vertical arrow marks the intersection with Line 3. The zig-zag line the lower crust of the velocity structure indicates a transitional zone within which velocity varies laterally. Assumed velocity in parentheses. See Fig. 4 for further explanation.

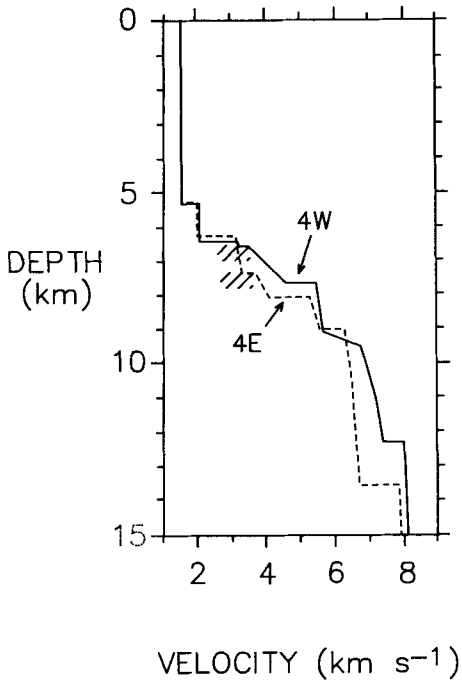

Figure 11. Velocity/depth profiles, at 15 km (4W) and 90 km (4E) from DOBS 1, through the model which best matches the synthetic seismograms. Hachures mark acoustic basement.

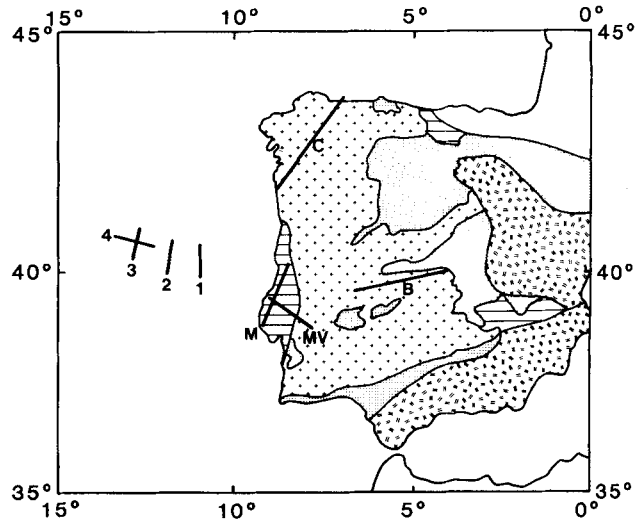

Figure 13. Location of land and sea seismic refraction profiles in western Iberia with respect to a regional geological map. +Iberian (Hercynian) Massif; = Alpine fold belts; dotted area, Tertiary basins; horizontal lines, Mesozoic basins. C = Cordoba *et al.* (1987), *B* = *Banda et al.* (1981), M = Moreira *et al.* (1982), MV = Mendes Victor *et al.* (1980). Lines 1–4 are reported here.

Mesozoic sediments have velocities in the range 4.0–5.0 km s^{-1}, the upper continental crustal velocity is 5.1–6.5 km s^{-1} and the lower crustal velocity does not exceed 6.9 km s^{-1}.

Although many seismic refraction studies have now been made of continental crust at non-volcanic rifted margins almost all modelling has been done using traveltimes alone giving velocity profiles which often have poorly constrained gradients. The only velocity structures well constrained by synthetic seismograms appear to be those of Duschenes, Sinha & Louden (1986), Whitmarsh *et al.* (1986) and LASE Study Group (1986). The first two are from eastern Sardinia and North Biscay, respectively. These margins resemble the western Iberian margin in being relatively sediment-starved margins. The principle feature of both models (Fig. 14a) is the absence of first-order changes in velocity in the crust and the approximation of the structure to a single linear, or slightly downward-decreasing, gradient. The different crustal thickness of the two models may be attributed to variations in crustal thinning. The LASE results, from the thickly sedimented eastern margin of the USA, did not clearly differentiate between oceanic and thinned continental crust and were unusual for rifted margins in indicating an extensive 7.2 km s^{-1} layer which was attributed to crustal underplating.

The seismic characteristics of mature oceanic crust, away from fracture zones and large seamounts and ridges, have been studied world-wide. The velocity structures have several common features which are independent of spreading rate but depend, in the upper crust, on age. White *et al.* (1984) gathered all available North Atlantic velocity structures which were based on synthetic seismogram modelling and found that, for crust over 50 Myr old, they fall within a quite narrow range (Fig. 14a). The envelope in

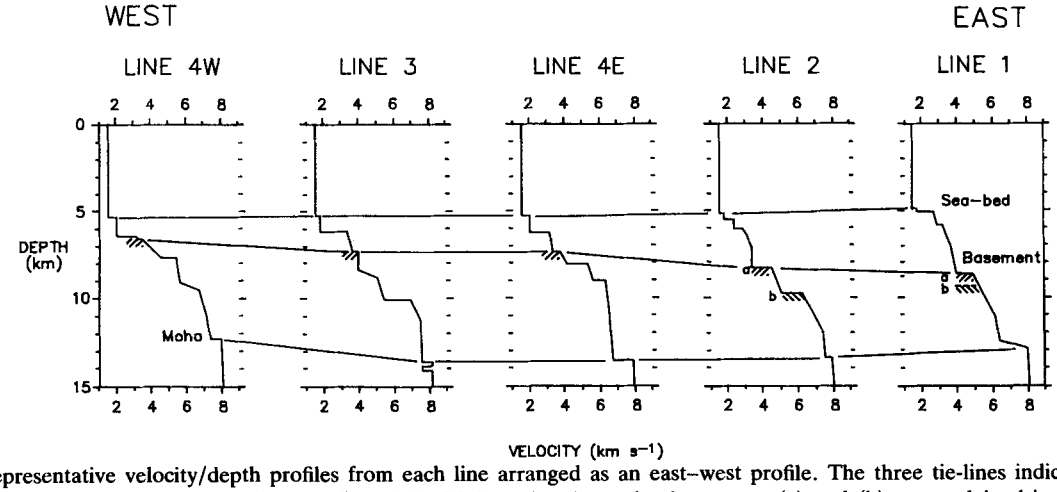

Figure 12. Representative velocity/depth profiles from each line arranged as an east–west profile. The three tie-lines indicate, from top to bottom, the seabed, acoustic basement (hachured) and the Moho. The alternative basements (a) and (b) are explained in the text. Line 1: profile taken 10 km from from DOBS 2; Line 2: profile taken 60 km from DOBS 2; Line 3: profile taken 15 km from DOBS 2.

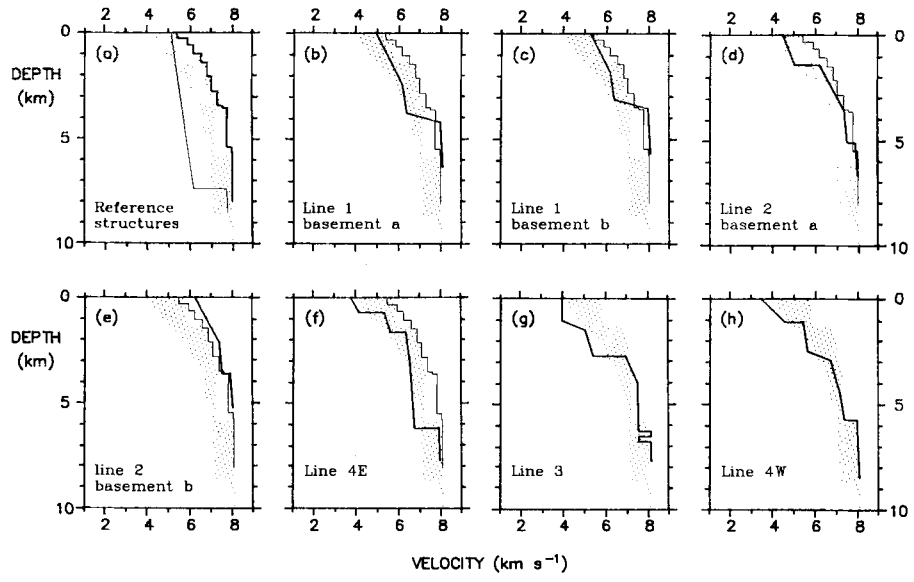

Figure 14. Interpretation of the velocity/depth profiles from Fig. 12 with respect to reference oceanic crust and thinned continental crust models based on synthetic seismogram modelling. (a) dots indicate the envelope of North Atlantic models for oceanic crust over 50 Myr old (White *et al.* 1984). Bold line is a model for thinned continental crust (with sediments omitted) from North Biscay (Whitmarsh *et al.* 1986); thin line is from Duschenes *et al.* (1986). The oceanic crust envelope and the North Biscay model are repeated throughout the figure for reference. (b) Line 1 structure relative to the depth of acoustic basement, horizon (a) in Fig. 12. (c) as (b) but referred to horizon (b) in Fig. 12. (d) Line 2 structure relative to acoustic basement. (e) as (d) but referred to horizon (b) in Fig. 12. (f), (g), (h) Line 4E, Line 3, Line 4W structures respectively relative to acoustic basement (see text).

Fig. 14(a) was used therefore as a yardstick for the recognition of oceanic crust.

Line 1. The top 4 km of the sub-basement velocity structure (Fig. 14b) falls within the oceanic bounds but the crust is too thin to be oceanic and the velocities characteristic of layer 3 (6.7–7.3 km s^{-1}) are completely absent. The crustal structure, in shape, gradient and thickness, is very like the North Biscay model but generally slower by about 0.8 km s^{-1}. The comparison is even better however if true basement is assumed to lie under about 0.7 km of (Mesozoic?) pre-rift sediment (with velocity 5.0–5.3 km s^{-1}); see Fig. 14(c) where the velocity profile has been raised by 0.7 km. Our conclusion is that Line 1 overlies thinned continental crust.

Line 2. Similar arguments as above can be applied to this line but in this case the velocity exceeds the oceanic bounds 3 km into basement (Fig. 14d). The lower part of the velocity structure is closely similar to the North Biscay model and if the upper 1.5 km thick layer (4.5–5.1 km s^{-1}) is equated with (Mesozoic?) pre-rift sediment the match in crustal thickness and velocity is very close (Fig. 14e). The 1.5 km thick 7.5 km s^{-1} layer at the base of the crust is unusual but seems to be required to satisfy both traveltime and amplitude constraints. Such a velocity is unknown beneath Western Iberia (see above). It may be attributed to underplating by molten material generated in the vicinity of the ocean–continent boundary (White & McKenzie 1989). We conclude that Line 2 also overlies continental crust, probably proximal to the ocean–continent boundary.

Line 4 (east). The velocity structure falls almost entirely within the oceanic limits and the crustal thickness is typically oceanic (Fig. 14f). The only noticeable deviation from the oceanic bounds is in the lowermost crust where the envelope is narrowest. The structure is unlike the thinned continental crust of North Biscay in the presence of almost 3 km of low velocity gradient crust with a velocity exceeding 6.7 km s^{-1}. The crust is also thicker than at Lines 1 and 2 so that if it were continental it would contradict the concept of continental crust systematically thinning oceanwards. We conclude therefore that the easternmost 30 km of Line 4 lies over oceanic crust. It follows that the ocean/continent boundary lies within the 40 km wide region between the east end of Line 4 and Line 2.

Lines 3 and 4 (west). In modelling Line 4 two different crustal structures were found and the transition between them was associated with a region of poor transmission in the lower crust and uppermost mantle. Line 3 lies just west of this region. At the intersection of the two lines the velocity profiles extracted from the models derived from traveltimes alone are very close (Figs 8, 10). Further, the independently modelled structures for each line, based on synthetic seismograms, are very similar; the main difference is the slightly faster and thicker lower crust of Line 3. For the above reasons these two lines are considered together.

When compared with the oceanic bounds (Figs 14g,h) both structures have an 'oceanic' thickness but the upper crust velocities are generally lower and the lower crust velocities slightly higher. On the other hand there is even less similarity with models of thinned continental crust. We conclude therefore that Lines 3 and 4 (west) lie over oceanic crust.

The velocity contrast between the upper (<5.7 km s^{-1}) and lower (>6.8 km s^{-1}) crust is not only relatively large but also relatively sharp. Such structures are characteristic of

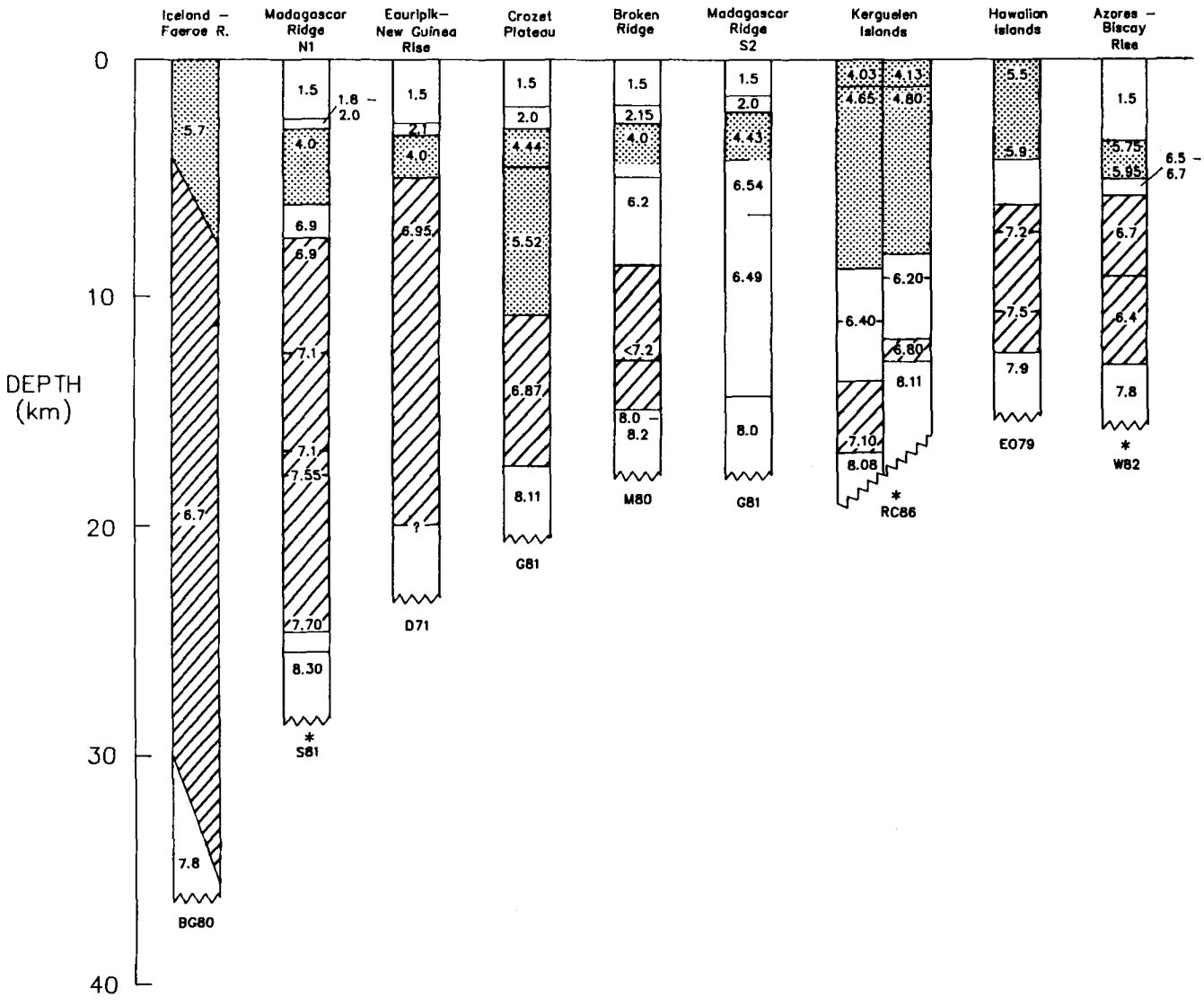

Figure 15. Compilation of velocity structures under hotspot or aseismic ridges. Stipple = up to 6.0 km s^{-1}; diagonal lines = 6.7–7.7 km s^{-1}. Asterisks denote structures based on synthetic seismograms.

so-called aseismic or hotspot ridges (Fig. 15) which are believed to result from localized excess volcanism during or after sea-floor creation. Even though the crust is not abnormally thick under Lines 3 and 4 (west) these lines do lie just north of the north end of the Madeira–Tore Rise, a suspected hotspot ridge (Morgan 1981).

Although we concluded above that the OCB lies between the east end of Line 4 and west of Line 2 we also found that no mantle arrivals were observed by any of the Line 4 DOBS for shots fired between DOBS 2 and 4. This may indicate an anomalous transition zone associated with the OCB. A 20 km wide zone of poor transmission is known to mark the OCB in the northern Bay of Biscay (Ginzburg *et al.* 1985).

INTERPRETATION OF MAGNETIC ANOMALIES

Magnetic anomalies in the vicinity of the seismic refraction lines were studied independently for evidence of the location of the ocean–continent boundary (OCB). At the same time it was hoped to clarify the relationship of the OCB with any sea-floor spreading magnetic anomalies of the M-series and to define further the age and nature of the J-anomaly (Pitman & Talwani 1972) and its associated basement ridge.

In order to compile an updated magnetic anomaly chart, data from Discovery Cruise 161 and elsewhere were appended to the NE Atlantic database of Verhoef *et al.* (1986). After some minor adjustments for cross-over discrepancies the resulting 19 825 point data set was regridded at 1.85 km and computer contoured. No correction was made to the data for diurnal variation which at this latitude on a quiet solar day can reach 30 nT (Regan & Rodrigues 1981). The Verhoef *et al.* (1986) data were taken as published.

The resulting contour chart shows three areas of different magnetic anomaly character (Fig. 16). Positive irregularly shaped anomalies of up to 250 nT in the NE quadrant are roughly bounded by the 5000 m isobath at the foot of the shoal area (minimum depth about 700 m) which includes Galicia Bank and the Vasco de Gama and Vigo seamounts. The western third of the chart and the SW corner are dominated by larger more linear anomalies of variable

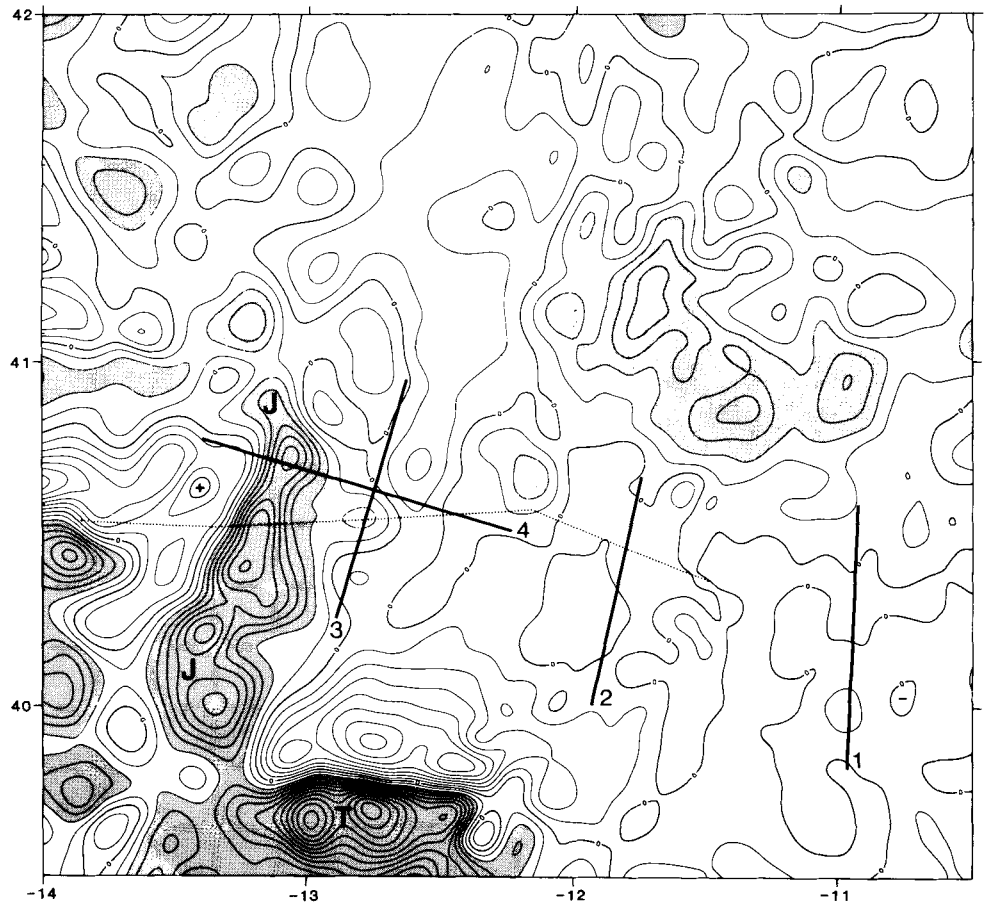

Figure 16. Magnetic anomaly chart of the study area (contour interval 50 nT); areas greater than 100 nT are shaded. Bold lines are refraction profiles reported here. Dotted line is the track of the modelled magnetic anomaly profile. J = J magnetic anomaly; T = Tore Seamount.

direction with amplitudes ranging from −350 to 600 nT. The pair of large E–W anomalies (T) in the south of this region is associated with Tore seamount. Adjacent to it is the large NNE-trending positive J-anomaly (J) which terminates in the vicinity of 41°N. The remaining central part of the chart shows an L-shaped area of low amplitude anomalies dominated by the random sinuosity of the zero nT contour.

The J-anomaly is associated with a basement ridge which extends north to about 41°20′N (Fig. 17). This ridge and Tore seamount are at the north end of the Madeira–Tore Rise, an aseismic or hotspot ridge often paired on plate-reconstructions with the J-anomaly ridge of the western north Atlantic (Tucholke & Ludwig 1982). Although the J-anomaly lies between anomalies M0 and M2, both south of the Newfoundland Fracture Zone (Tucholke & Ludwig 1982) and in the vicinity of the Madeira–Tore Rise south of the Azores–Gibraltar Fracture zone (Rabinowitz, Cande & Hayes 1979), it is not clearly established as an isochron off Iberia or east of the Grand Banks. However the fact that the J-anomaly is subparallel to anomaly 34 on both sides of the Atlantic plus its termination at latitude 41°N in the Iberia Abyssal Plain and just north of the Newfoundland seamounts (Meador & Austin 1988), suggests that the J-anomaly formed by sea-floor spreading at a northward-propagating spreading centre (Masson & Miles 1984) i.e. it *is* an isochron. Indeed, the J-anomaly has been interpreted by several authors as an isochron which also marks the onset of sea-floor spreading between Iberia and the Grand Banks (Sullivan 1983; Klitgord & Schouten 1986; Meador, Austin & Dean 1988).

To investigate the crustal structure from the magnetic signature in the vicinity of the seismic refraction lines an anomaly profile was 'constructed' from a pair of intersecting roughly E–W tracks (Fig. 16). The profile was projected onto an azimuth of 113°, parallel to a linear trough in the acoustic basement south of Galicia Bank (Fig. 17). This we interpret as the fracture zone inferred to exist by Boillot & Winterer (1988); its trend provides the best estimate of spreading direction. Magnetic models were constructed on the assumption of a 2-D structure extending to infinity in a direction normal to the profile. Depth to acoustic basement was calculated from a time-section picked off the contoured basement chart and from interval velocities obtained from sonobuoy 2 (Table 1). A remanence vector for offshore the Iberian margin was calculated from the Cretaceous palaeopole position for Eurasia at 110 Myr BP (Irving & Irving 1982). This included a 25° clockwise rotation of Iberia, somewhat less than the 34° total post-late Jurassic rotation of Iberia (Galdeano *et al.* 1989).

The 'observed' magnetic anomaly profile shows the dominance of the J-anomaly and the 'flatness' of the easternmost 80 km of the profile (Fig. 18a). A number of hypotheses was tested. An initial constraint is that, given the normally very low magnetization of continental crust (typically less than $2\,A\,m^{-1}$), and assuming acoustic basement corresponds to the top of the igneous or metamorphic crust, it is not possible for such crust to extend west of about 120 km on the observed profile because of the

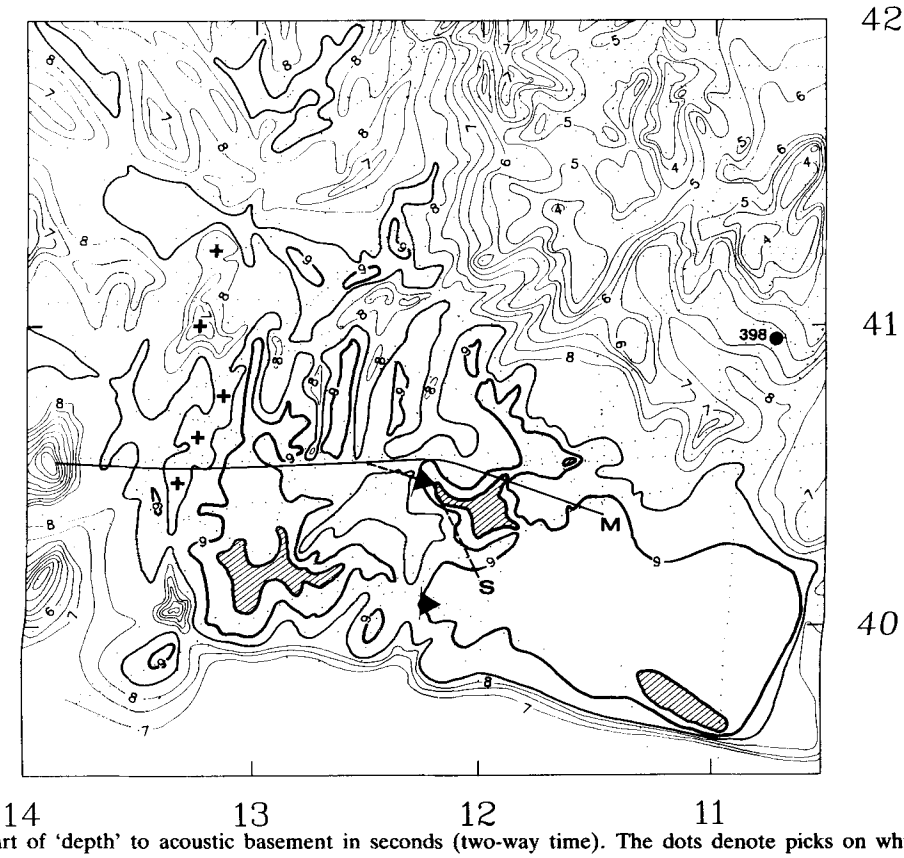

Figure 17. Contour chart of 'depth' to acoustic basement in seconds (two-way time). The dots denote picks on which the contouring was based. Contours greater than 8 s are bolder. The triangular symbols denote places where the basement abruptly deepens landward (see text). + signs denote the ridge associated with the J-anomaly. 398 denotes DSDP Site 398. Sources, Discovery Cruise 161 plus data from Ifremer Centre de Brest, Institut Français de Pétrole, University of Utrecht. M = Magnetic profile in Fig. 18; S = reflection profile in Fig. 19.

relatively large observed anomalies. Higher magnetizations can occur in continental crust associated with intrusions or mineralization but they are usually localized on the scale of a few kilometres (Talwani & Eldholm 1972). For simplicity we have assumed a 2 km thick uniformly magnetized source layer to represent thinned continental crust. Alternatively a higher magnetization, typical of *c.* 110 Myr oceanic crust, can be used to model the likely effect of constantly polarised relief on the top of oceanic layer 2. Dredged and drilled oceanic basalts away from spreading centres typically have magnetization of about $4\,A\,m^{-1}$ (Lowrie 1977). In the North Atlantic higher values (about $10\,A\,m^{-1}$) have been found in the vicinity of anomally M0 (Donnelly *et al.* 1979). The thickness of the magnetized layer in the oceanic crust is arguable (Lowrie 1979; Banerjee 1984; Vogt 1986). Although the basalt layer may be only 1.5 km thick there is evidence that the underlying much thicker, but less intensely magnetized, gabbros contribute significantly (Lowrie 1977). Here a compromise was reached by assuming a single 2 km thick source layer with a magnetization of $8\,A\,m^{-1}$. Basement relief alone, although producing anomalies of the correct shape and wavelength, is insufficient to produce large enough anomalies and higher intensities and/or magnetization contrasts are required.

Recently, the J-anomaly between Iberia and the Grand Banks has been equated with anomaly M0 (Srivastava *et al.* 1988). This hypothesis was tested for the Iberia Abyssal Plain using the geomagnetic reversal chronology of Kent & Gradstein (1986). We chose spreading rates to emulate the observed profile and a relatively high magnetization adjacent to the older M0 reversal to model the J-anomaly. A rather low spreading-rate model of $5\,mm\,yr^{-1}$ [the average rate between anomalies 34 and J (M0) is $8\,mm\,yr^{-1}$] shows a maximum at the J-anomaly location but the amplitude and shape of the sequence is a poor match (Fig. 18c). In addition, the implied onset of sea-floor spreading (135 Myr) is significantly earlier than indicated by the deep drilling results at Site 398 (113 Myr; Boillot & Winterer 1988). Spreading rates of 9.5 and $11\,mm\,yr^{-1}$ imply initiation of spreading at about the beginning of chron M3 around 124–125 Myr. There is quite good matching of wavelengths and amplitudes (Fig. 18b and c). As well as the M0 anomaly the other distinctive features caused by the M-series anomalies are the low 'saddle' east of the J-anomaly (Model c) and the *c.* 200 nT deep trough over anomaly M3 (Models b and c). The small trough over the M1/M2 boundary is not clearly observed either in the observed profile or as a lineation on the contour chart (Fig. 16); it may have been missed due to its relatively small amplitude.

An equally convincing, but less objective, model is produced by the hypothesis that all the oceanic crust along the profile was created during the constant normal polarity interval following anomaly M0, i.e. it is post-118 Myr in age (Kent & Gradstein 1986), and that the observed anomalies are due to variations in intensity, but not polarity, within the crust (Fig. 18d). This model has continental crust east of 142 km, a rather high magnetization of $18\,A\,m^{-1}$ at the

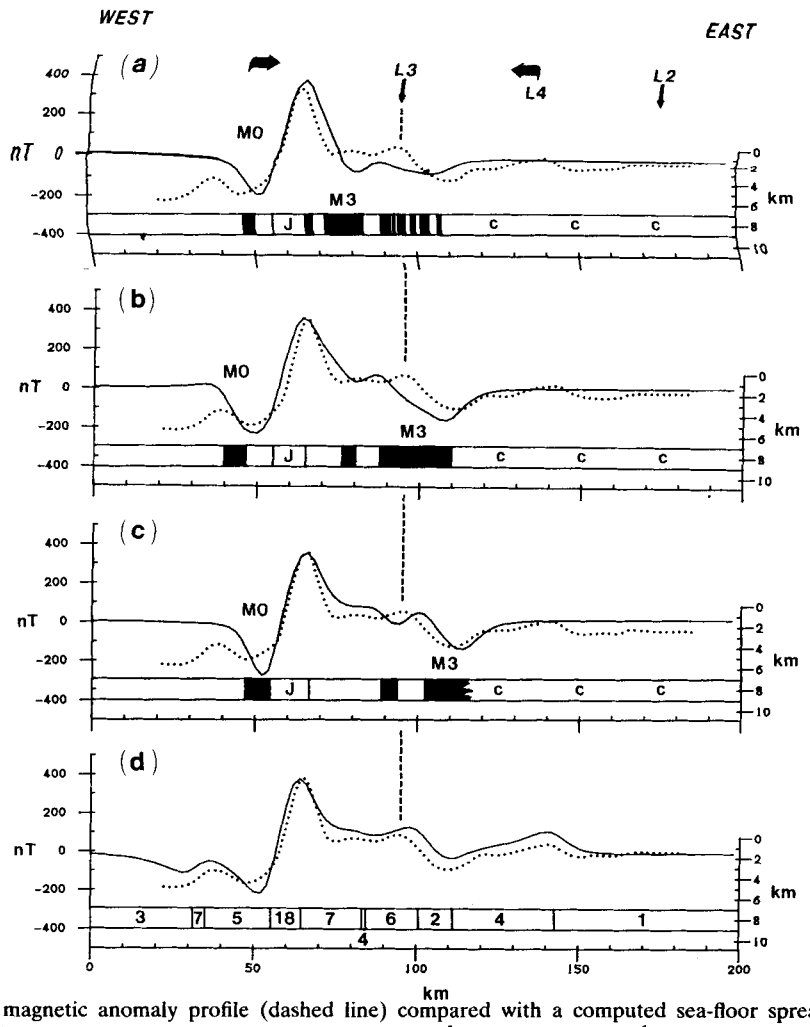

Figure 18. (a) Observed magnetic anomaly profile (dashed line) compared with a computed sea-floor spreading model from M0 to M10 spreading at 5 mm yr^{-1}. The oceanic crust has a magnetization of 8 A m^{-1} (except J, 12 A m^{-1}), reversed polarity blocks are dark. The J-block was located to give the best fit to the observed profile. Continental crust labelled 'c' has a uniform magnetization of 1 A m^{-1}. Induced magnetization was not included in the model as it is normally an order of magnitude weaker than remanent magnetization in oceanic basalts (Lowrie 1974; Ryall *et al.* 1977). (b) As (a) but for sea-floor spreading from M0 to M3 at 9.5 mm yr^{-1}. (c) As (b) but spreading at 11 mm yr^{-1} starting *within* the M3 reversed polarity period. (d) As (a) but with a computed profile due to a variably magnetized basement (1 to 18 A m^{-1}) of constant polarity with a high magnetization associated with the J-anomaly.

J-anomaly ridge and varying but less intense magnetization elsewhere. The minimum spreading rate required between the OCB and anomaly 34 to support this model is 10.5 mm y^{-1}.

Models b, c and d all seem to fit the observed profile well and from magnetics alone we cannot discriminate between them (but see below). They do indicate however that continental crust must lie east of the 142 km position on the profile i.e. east of 40°35′N, 12°08′W (Figs 16 and 18). The model profiles also indicate that the existence of continental crust west of 110 km is most unlikely.

MORPHOLOGY OF ACOUSTIC BASEMENT

The remaining data set, which potentially could provide information about the location of the ocean–continent boundary, was the large number of mostly single channel seismic reflection profiles which had been collected over the eastern Iberia Abyssal Plain and the lower slopes of Galicia Bank and the adjacent continental margin. The shape of acoustic basement, assuming it represents the top of the igneous oceanic crust or the top of the pre-rift continental crust, can provide useful evidence about the nature and tectonics of the crust. Thus all available profiles were obtained and acoustic basement picked out wherever possible. On some profiles the sediment was too thick and the basement signal too weak for this to be possible. Only in the southeast corner of the chart was it consistently impossible to pick acoustic basement; here it is at least 9 s deep everywhere. The resulting 'depths' were hand-contoured to generate Fig. 17.

The Galicia Bank block occupies the northeast corner of the chart. The southern edge of the chart is marked by the steep northern flank of the Estremadure Spur which may represent the western extension of the Nazaré Fault (Mougenot 1988). This feature also seems to be the northern limit of the broad zone of current seismicity associated with the convergence of Iberia and Africa (Grimison & Chen 1988).

A probably significant feature is the 113° trending trough which extends at least 150 km WNW from 41°10′N, 12°W. This trough truncates several other ridges and troughs at

high angles and is approximately colinear with the southern boundary of the Galicia Bank block. The trend is also very close to the 106° trending flow lines calculated by Sibuet *et al.* (1987) for the initial opening between Iberia and the Grand Banks. Thus there is a strong suggestion that the trough represents an original fracture zone present at the initiation of sea-floor spreading. We call this the Figueira Fracture Zone after the Portuguese coastal town which lies on the eastward extrapolation of the fracture zone.

Immediately south of the fracture zone there is a series of roughly north–south-trending ridges and troughs, with an average ridge-to-ridge spacing of about 20 km, which persist almost as far east as 12°W. The J-anomaly ridge, at about 13°20′W, is the most extensive of these features. Further east the north–south trend dies out south of 40°30′N.

The final characteristic of the basement chart is the general southward deepening of acoustic basement beneath the abyssal plain. This is evident not only on the chart but also along refraction lines 1, 2 and 3 (Figs 4, 6 and 8 respectively) which were roughly along the strike of the basement. It is conceivable that this deepening is the result of deformation related to one or more of the roughly north–south Cainozoic compressional episodes suffered by the region.

Further evidence of the location of oceanic and thinned continental crust may be available from the depth to basement. The seismic refraction results (Fig. 12) indicate that thinned continental crust under Lines 1 and 2 (at most 4–5 kms thick) is always thinner than the adjacent oceanic crust (*c.* 6 km). Assuming at the initiation of sea-floor spreading that both crusts were in isostatic equilibrium this implies that originally the top of continental basement was only about 100 m deeper than the ocean crust if the average densities (2.89 and 2.80 g cm^{-3}) of normal oceanic and continental crust are used respectively (Carlson & Raskin 1984; Barton 1986). However if at that time the 'oceanic' crust was erupted in shallow water, or even subaerially, then a lower crustal density will apply due to the presence of more vesicular lavas. For example a mean density of 2.75 g cm^{-3} implies a depth difference of 450 m (perhaps 0.3 to 0.4 s TWT). Alternatively, or additionally, the thinned continental crust adjacent to the OCB may have an unusually high density if it has been intruded by dykes (perhaps associated with the underplating suggested under Line 2) and this too will tend to increase the depth differential. Thus, if the above arguments hold, one may expect a relatively rapid increase landward in the depth to basement as the OCB is crossed.

The OCB in the Tagus Abyssal Plain, although located primarily according to the seaward disappearance of a landward-dipping deep crustal reflector (Mauffret *et al.* 1990), lies just west of a deep linear basement trough thereby fitting the above criterion. A similar depth difference has been observed on the margin west of Galicia Bank (Maufret & Montadert 1987). Meador & Austin (1988) also located the OCB on a profile just north of the Newfoundland Seamounts, on the conjugate margin to that described here, at a point where acoustic basement abruptly deepens landward by about 1 s TWT. In the Iberia Abyssal Plain a rapid basement deepening is also visible on at least two of our three east–west reflection profiles (Figs 2, 17, 19). Unfortunately the clarity of the basement reflector is uneven in our data and this technique for detecting the OCB is qualitative and not well substantiated. However it is remarkable that estimates of the OCB location, based on the two southernmost reflection profiles, fall very close to locations based on other geophysical criteria.

DISCUSSION

The primary objective of the work described here was to locate the ocean–continent boundary (OCB) in the eastern Iberia Abyssal Plain. We have obtained estimates of this location based on three independent geophysical criteria. The seismic velocity structure of the lower crust indicates that the western edge of thinned continental crust occurs within a 35 km wide zone between the east end of Line 4 and Line 2 at about 12°W and that the eastern half of Line 4 is over a region of poor transmission in the uppermost mantle which may coincide with an ocean–continent transition zone (Fig. 2). Modelling of a single magnetic anomaly profile roughly along Line 4 (Fig. 18) locates the easternmost strongly magnetized oceanic crust about 50 km east of the J-anomaly peak i.e. at 40°34′N, 12°30′W. The magnetic anomaly chart also indicates that generally the anomaly amplitude is very low east of about 12°10′W (Fig. 16). Lastly, abrupt landward increases in the depth to acoustic basement on two east–west reflection profiles indicate a substantial change in crustal thickness and/or density, which could be associated with the OCB, at about 12°15′W (Figs 17, 19). The above three sets of observations are summarized in Fig. 20. The widest limits on the OCB position at 40°30′N are therefore 12°10′ and 12°30′W from the magnetics and the seismic structure suggests that there may be a transition zone within these limits.

Although the strike of the OCB is clearly roughly north–south evidence of its precise orientation is weak. The ridges and troughs in the oceanic basement strike about 010° (Fig. 17) and the magnetic anomaly contours about 018° (Fig. 16). Either direction is roughly normal to the Figueira fracture zone trough at 41°N. We adopt an 010° direction because it is better defined by the series of relatively short-wavelength basement features. The along-strike continuity of the OCB is even more difficult to ascertain. The essential continuity of the J-anomaly and its associated ridge, the absence of another basement trough like that at 41°N and of any substantial traveltime anomalies along Line 3 are strong arguments that any offsets in the OCB are small (less than about 15 km). The apparent disappearance of the linear ridges and troughs in the oceanic basement south of 40°35′N is puzzling but by itself is not necessarily evidence of a fracture zone. We simply assume continuity of the OCB between the Figueira fracture zone and the Estremadure Spur because contrary evidence is inconclusive. Fig. 20 also includes locations of the OCB off Galicia Bank. The Galicia Bank margin has been extensively investigated by dredging, submersible sample and deep scientific drilling as well as by conventional geophysical techniques. The evidence for the OCB was summarized recently by Sibuet *et al.* (1987). Unreversed seismic refraction and multichannel seismic reflection profiles, magnetic anomalies and drilling results indicate that the ocean–continent transition lies just west of the serpentinized peridotite hill at 42°01′N, 12°53′W. The strike of the OCB and peridotite ridge is close to

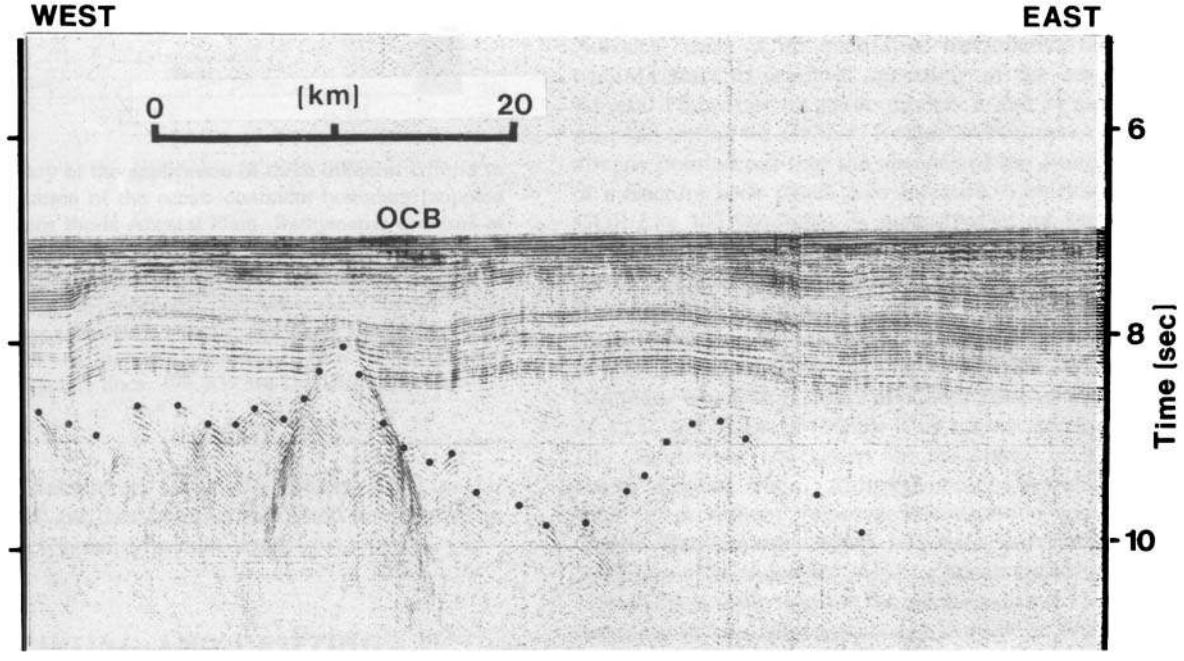

Figure 19. Reflection profile showing the abrupt increase in depth to acoustic basement (dots) on crossing the ocean–continent boundary (OCB) from west to east. See Figs 2 and 17 for location.

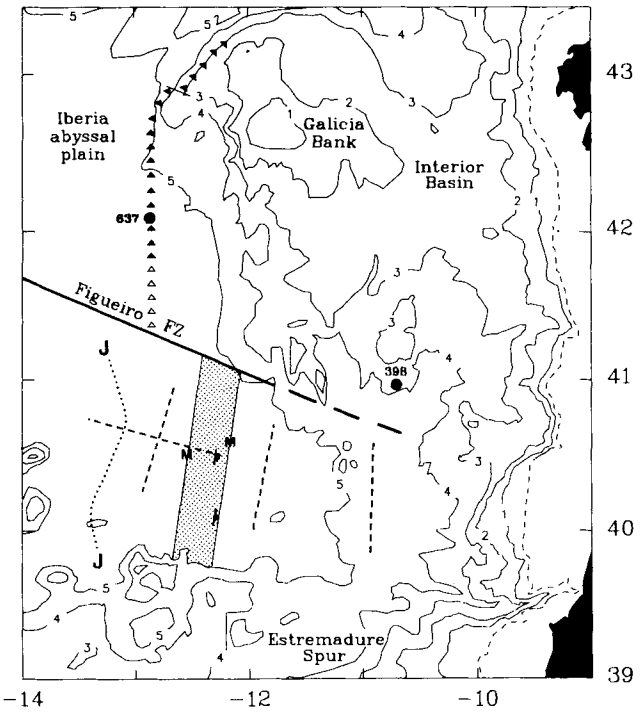

Figure 20. Summary of the application of three different criteria to estimating the location of the ocean–continent boundary (stippled band) in the eastern Iberia Abyssal Plain. Bathymetric contours at 200 and 1000 m and then every 1000 m. Solid/open triangles denote firm/uncertain ocean–continent boundaries respectively (Boillot & Winterer 1988); J = J magnetic anomaly; M = bounds from magnetic modelling (see text); triangle and bar = abrupt landward incease in depth of acoustic basement (see text); dashed lines = seismic refraction lines. 398, 637 are DSDP/ODP sites.

north–south (Thommeret, Boillot & Sibuet 1988) as far south as 41°40'N and has been extrapolated southwards in Fig. 20 up to the Figueira fracture zone.

TIMES OF RIFTING AND DRIFTING

Only our magnetic data has the potential to provide estimates of the age of important events in the eastern Iberian Abyssal Plain and strictly it relates just to the history of sea-floor spreading there. Careful modelling of a single magnetic anomaly profile indicates that sea-floor spreading is unlikely to have begun before chron M3 and could even have started after the end of anomaly M0 (but see below).

The above estimates must be consistent with other evidence and in particular that from Deep-Sea Drilling Project (DSDP) Site 398 and Ocean Drilling Program (ODP) Sites 637–641 off Galicia Bank. Sites 638, 639 and 641 were drilled on a tilted fault block and sampled syn-rift and post-rift sediments. The boundary between the two lies at the top of the Aptian sequence (Boillot & Winterer 1988). This boundary is also correlated with a regional break-up unconformity seen on reflection profiles. At Site 641 the boundary lies 40 m above the magnetic reversal which ends the M0 interval (Ogg 1988) and is therefore well within the Cretaceous constant polarity interval. If the earliest post-rift sediments are synchronous with the onset of sea-floor spreading then the absence of anomaly M0 west of Galicia Bank is explained. Site 398 was drilled near the southern end of Vigo Seamount which is now known to be over 100 km landward of the OCB. Site 398 is probably on the same continental 'block' at Sites 638–641 since it lies north of the landward extension of the Figueira fracture zone. The syn-rift/post-rift boundary appears to lie between acoustic or seismic formations 3 and 4 (Groupe Galice 1979). This was correlated with a downhole Aptian/Albian unconformity at 1400 m depth (Sibuet *et al.* 1979). The magnetic stratigraphy of the cores down to 1737 m depth strongly suggests that polarity interval M0 is absent, thereby appearing to confirm the acoustic and biostratigraphic correlation, although sampling was not entirely continuous (Morgan 1979).

Thus there appears to be agreement between Sites 398 and 641 as to the age of the syn-rift/post-rift boundary off Galicia Bank which we assume was contemporary with the onset of sea-floor spreading. Further, assuming the widely accepted south-to-north separation of Iberia and North America, there is no qualitative discrepancy between the post-M4 start to sea-floor spreading in the eastern Iberia Abyssal Plain (our magnetic models b and c) and the later post-M0 timing off Galicia. Boillot & Winterer (1988) have already pointed out that the absence of the J-anomaly north of a fracture zone which they inferred to exist south of the ODP Leg 103 boreholes is suggestive of an age difference for the onset of sea-floor spreading on either side of it. On the basis of our magnetic models b and c, i.e. assuming that the J-anomaly just pre-dates M0, as it does south of 35°N in the east Atlantic (Rabinowitz *et al.* 1979), this age difference is that between 125 or 124 Myr BP and the Aptian–Albian boundary which is 11 to 12 Myr according to the time-scale of Kent & Gradstein (1986). This time-scale also implies a late Hauterivian break-up unconformity in the eastern Iberia Abyssal Plain. Although borehole data is lacking there a prominent regional unconformity exists on the Galicia Bank margin which has been correlated with the boundary that separates upper syn-rift sediments (seismic Unit 4) from lower syn-rift sediments (seismic Unit 5) and is therefore of late Hauterivian age (Boillot & Winterer 1988; Mauffret & Montadert 1988). We do not know whether this is a coincidence or whether, as sea-floor spreading propagated northwards, its onset in one ridge segment was recorded in the next adjacent, but still rifting, segment.

The above discussion demonstrates the consistency of our magnetic models b and c, which date the J-anomaly as just older than M0, with events off Iberia. A new feature of the models however is the implication that drifting began in Late Hauterivian time. This is 11 to 12 Myr earlier than off Galicia Bank where in turn drifting began about 6 Myr earlier than off Goban Spur. This rather large difference of 11 to 12 Myr between two adjacent segments of margin is surprising but may reflect the fact that a break-up unconformity and the onset of sea-floor spreading in a magnetic model are measures of two different effects which occur at different times in the rifting/drifting process.

Magnetic model d is not only subjective but also differs from earlier work, based on observations south of 35°N in the east Atlantic, in assigning J to the Cretaceous constant polarity interval.

A post-M0 onset for sea-floor spreading in the Iberia Abyssal Plain would pre-date the same event off Galicia Bank by not more than 5 Myr and therefore, at first, seems more plausible than the 12 Myr delay inferred by models b and c. The evidence at present however seems to favour the latter models.

IMPROVING THE FIT OF IBERIA TO NORTH AMERICA

It is beyond the scope of this paper to propose, quantitatively and in detail, a new reconstruction of Iberia and North America which takes account of the location of the OCB off Iberia described here. However it is appropriate to discuss qualitatively some of the resulting implications for such reconstructions.

Firstly the above history of events off Iberia is compatible with out less extensive knowledge of the conjugate Grand Banks margin. The J-anomaly and its basement ridge can be traced as far north as 45°40'N, several hundred kilometres north of the Newfoundland seamounts, the probable conjugate of the Estramadure Spur (Srivastava *et al.* 1988; Meador & Austin 1988). The ocean–continent boundary has been recognized on multichannel seismic reflection profiles and lies at least 150 km landward of anomaly J (Keen & de Voogd 1988). A prominent late Early Cretaceous unconformity on the Grand Banks can be traced seaward to the vicinity of the J-anomaly just north of the seamounts where it onlaps acoustic basement (Meador *et al.* 1988).

Plate reconstructions of Iberia and North America have previously attempted to match conjugate sea-floor spreading anomalies [e.g. anomaly M0 by Srivastava *et al.* (1988)] or inferred OCB's (e.g. Masson & Miles 1984). So far no account has been taken of the thinning, and consequent extension, of the continental crust as was done, for example, by Dunbar & Sawyer (1987) for the Gulf of Mexico. Reconstructions which fix Flemish Cap rigidly to the Grand Banks and Galicia Bank to Iberia, respectively, always show Flemish Cap in contact with Galicia Bank. This invariably leaves an open region to the southwest, corresponding to the western Newfoundland Basin and the eastern Iberia and Tagus Abyssal Plains. The most successful reconstruction based on magnetic anomalies seems to be that of Srivastava *et al.* (1988) which equates the J-anomaly with the M0 isochron and also matches, within about 100 km, the north end of the J-anomaly on either side of the Atlantic (Fig. 21a). Our new data suggest that such reconstructions should pre-date anomaly J.

The OCB off the eastern margin of the Grand Banks (Keen & de Voogd 1988) has a marked sinuousity at a point which could be construed to be in line with the Figueira fracture zone [see dots in Fig. 21(a)]. Off Flemish Cap the OCB location is apparently poorly constrained and the overlap in Fig. 21(a) probably reflects this uncertainty. In any event the Canadian OCB clearly converges with anomaly M0. Off Iberia the evidence is less clear because the strike of the individual OCB segments is weakly constrained. However in general the location of these segments is consistent with a northward convergence of the OCB and the J-anomaly. Thus we agree with Srivastava *et al.*'s (1988) conclusion that sea-floor spreading propagated northwards along the Iberia/Grand Banks margins. The question remains as to whether the Canadian OCB can be matched to the OCB off Iberia. A speculative qualitative fit, involving a 16° rotation with respect to Fig. 21(a) and the matching of the Iberia Abyssal Plain OCB and its conjugate, is shown in Fig. 21(b). Consequences of this reconstruction are (a) overlap of Flemish Cap and Galicia Bank and (b) failure of the OCB's to match in the Tagus Abyssal Plain. Thus, although we attribute the mismatch of the Tagus Abyssal Plain OCB to an incorrect location of the OCB there, the overlap is a problem. It may be accommodated by post-M0 crustal thinning landward of the two banks, and/or by uncertainties in the OCB location off Flemish Cap.

In addition Fig. 21(b) does not take account of crustal stretching. Judging by our seismic refraction results (Fig. 12) and the elevation of Galicia Bank, crustal stretching in the eastern Iberia Abyssal Plain was greater than off Galicia Bank (even allowing for stretching beneath the Interior

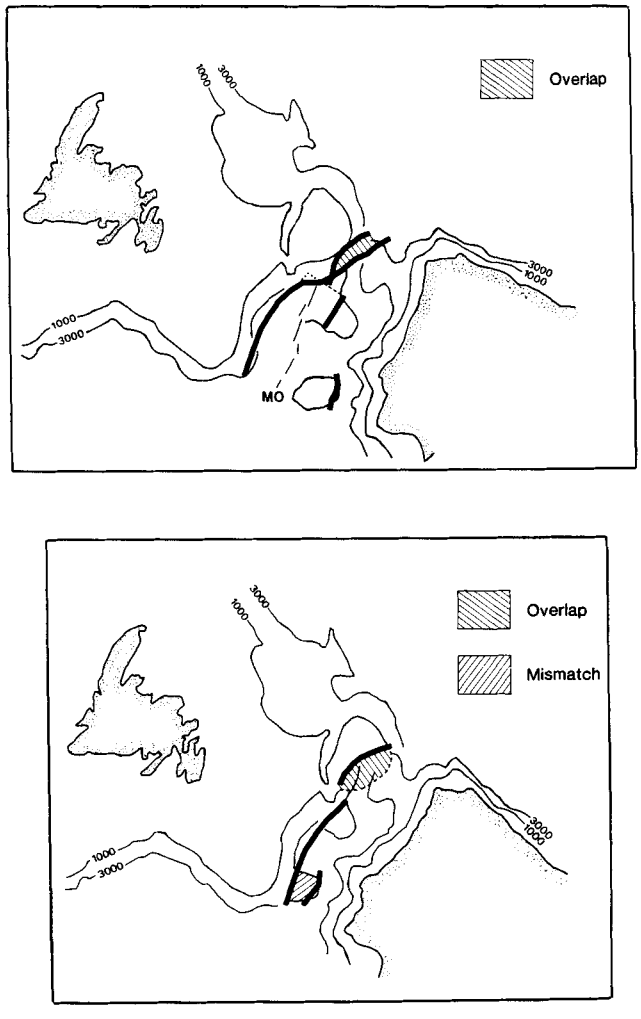

Figure 21. (a) The M0 reconstruction of Srivastava *et al.* (1988). Bold lines are OCB's from Keen & de Voogd (1988), Boillot & Winterer (1988), this paper and Mauffret *et al.* (1990). The dotted line represents an alternative interpretation consistent with the existence of the Figueiro fracture zone. (b) A qualitative and speculative fit of the Iberian and North American OCB's achieved by taking the M0 reconstruction in Fig. 21(a) and rotating Iberia 16° with respect to North America. No palinspastic reconstruction of the continental margins has been attempted.

Basin). A similar, but more tentative, conclusion may be reached by comparing the shallow Flemish Cap, which probably lies close to the OCB on its southeast margin (Fig. 21a), with the wider shelf-to-OCB region just south of 45°N. Thus ultimately a tight pre-rift fit of the eastern Grand Banks margin to Iberia seems to be impossible. Either Flemish Cap and/or Galicia Bank moved independently of their 'parent' continents in pre-M0 time or else the OCB identifications are greatly in error.

The relatively small amount of crustal thinning between Flemish Cap and Galicia Bank is explained as follows. By M0 time (Fig. 21a) sea-floor spreading had propagated only as far north as the Figueiro fracture zone north of which limited crustal thinning had occurred. Thinning, however, was sufficient to provide a zone of weakness which failed completely when the relative Iberia–North America plate-motions 'abruptly' changed direction at about M0 time (Srivastava & Tapscott 1986). It is possible that this unusual scenario could explain the widespread occurrence of peridotite along the western margin of Galicia Bank (Boillot & Winterer 1988).

CONCLUSIONS

(1) Three independent geophysical criteria provide overlapping constraints on the location of the ocean–continent boundary (OCB) in the eastern Iberia Abyssal Plain and suggest it lies close to 40°30'N, 12°15'W (Fig. 20), possibly within a transition zone from 12°10' to 12°30'W.

(2) The OCB extends in a roughly 010° direction continuously for 130 km without detectable offset. The southern limit is set by the east–west Estremadure Spur. At its north end the OCB is offset up to 70 km westwards by the newly discovered Figueira fracture zone.

(3) The J magnetic anomaly is also truncated by the Figueira fracture zone and is not detected further north. Magnetic anomaly modelling suggests sea-floor spreading in the eastern Iberia Abyssal Plain began at or just after the beginning of chron M3 (late Hauterivian; Kent & Gradstein 1986), some 11 to 12 Myr before it began off Galicia Bank.

(4) The newly discovered location of the OCB beneath the eastern Iberia Abyssal Plain largely solves the problem of the origin of the gap at that latitude in many first-order reconstructions of Iberia and North America, viz. a large deep-water area is underlain by highly attentuated continental crust.

(5) The following geophysical criteria were used to identify the OCB and may be successfully used elsewhere on non-volcanic rifted margins:

(a) the seismic structure of the lower crust. The North Biscay model of thinned continental crust (Whitmarsh *et al.* 1986) proved to be an excellent discriminant for differentiating thinned continental crust from normal oceanic crust;

(b) the relatively low remanent magnetization of continental crust compared to oceanic crust;

(c) an abrupt increase in depth to acoustic basement on passing from oceanic to thinned continental crust at the OCB. There are reasons to expect such a change in some circumstances (see text) but, pending further research, this criterion should be used with caution.

ACKNOWLEDGMENTS

We thank the officers and crew of Discovery Cruise 161 and our RVS colleagues for their assistance in collecting the data reported here. Bob Kirk and Martin Saunders were responsible for recording and processing the excellent OBS data. Doug Masson provided a most useful critique which helped to improve our arguments. We thank J. C. Sibuet and B. Collette for freely providing additional magnetic data. A.M. thanks the Conseil National de Recherche Scientifique for support. Institute of Oceanographic Sciences Deacon Laboratory Contribution No. 90024.

REFERENCES

Banda, E., Surinach, E., Aparicio, A., Sierra, J. & Ruiz De La Parte, E., 1981. Crust and upper mantle structure of the central Iberian Meseta (Spain), *Geophys. J. R. astr. Soc.*, **67,** 779–789.

Banerjee, S. K., 1984. The magnetic layer of the ocean crust—how thick is it?, *Tectonophysics*, **105,** 15–28.

Barton, P. J., 1986. The relationship between seismic velocity and density in the continental crust—a useful constraint?, *Geophys. J. R. astr. Soc.*, **87,** 195–208.

Boillot, G., Winterer, E. L., Meyer, A. W. & Shipboard Scientific Party, 1987. *Initial Reports ODP 103,* US Government Printing Office, Washington, DC.

Boillot, G. & Winterer, E. L., 1988. Drilling on the Galicia margin retrospect and prospect, *Sci. Results, ODP 103,* pp. 809–828, US Government Printing Office, Washington, DC.

Carlson, R. L. & Raskin, G. S., 1984. Density of the ocean crust, *Nature,* **311,** 555–558.

Chapman, C. H. & Drummond, R., 1982. Body wave seismograms in inhomogeneous media using Maslov asymptotic theory, *Bull. seism. Soc. Am.*, **72,** 5277–5317.

Cordoba, D., Banda, E. & Ansorge, J., 1987. The Hercynian crust in north western Spain: a seismic survey, *Tectonophysics,* **132,** 321–333.

Donnelly, T., Francheteau, J. *et al.*, 1979. *Initial Reports of the Deep Sea Drilling Project, 51, 52, 53,* Part 2, US Government Printing Office, Washington, DC.

Dunbar, J. A. & Sawyer, D. S., 1987. Implications of continental crust extension for plate reconstruction: an example from the Gulf of Mexico, *Tectonics,* **6,** 739–755.

Duschenes, J., Sinha, C. & Louden, K. E., 1986. A seismic refraction experiment in the Tyrrhenian Sea, *Geophys. J. R. astr. Soc.*, **85,** 139–160.

Galdeano, A., Moreau, M. G., Pozzi, J. P., Berthou, P. Y. & Malod, J. A., 1989. New palaeomagnetic results from Cretaceous sediments near Lisboa (Portugal) and implications for the rotation of Iberia, *Earth planet. Sci. Lett.*, **92,** 95–106.

Ginzburg, A., Whitmarsh, R. B., Roberts, D. G., Montadert, L., Camus, A. & Avedik, F., 1985. The deep seismic structure of the northern continental margin of the Bay of Biscay, *Ann. Geophys.*, **3,** 499–510.

Grimison, N. L. & Chen, W. P., 1988. Source mechanisms of four recent earthquakes along the Azores–Gibraltar plate boundary, *Geophys. J.*, **92,** 391–401.

Groupe Galice, 1979. The continental margin of Galicia and Portugal, acoustic stratigraphy, dredge stratigraphy and structural evolution, *Initial Reports Deep-sea Drilling Project,* 47, part 2, pp. 633–662, US Government Printing Office, Washington, DC.

Irving, E. & Irving, G. A., 1982. Apparent polar wander paths Carboniferous through Cenozoic and the assembly of Gondwana, *Geophys. Surv.*, **5,** 141–188.

Keen, C. E. & de Voogd, B., 1988. The continental-ocean

boundary at the rifted margin off eastern Canada: new results from seismic reflection studies, *Tectonics*, **7**, 107–124.

Kent, D. V. & Gradstein, F. M., 1986. A Jurassic to recent chronology in the western North Atlantic region, in *Geology of North America*, vol. M, chapter 3, pp. 45–50, eds Vogt, P. R. & Tucholke, B. E., Geol. Soc. Am., Boulder, CO.

Kirk, R. E., Langford, J. J. & Whitmarsh, R. B., 1982. A three component ocean bottom seismogram for controlled source and earthquake seismology, *Mar. geophys. Res.*, **5**, 327–341.

Klitgord, K. D. & Schouten, H., 1986. Plate kinematics of the central Atlantic, in the western North Atlantic region, in *Geology of North America*, vol. M., chapter 22, pp. 351–378, eds Vogt, P. R. & Tucholke, B. E., Geol. Soc. Am., Boulder, CO.

LASE Study Group, 1986. The structure of the US East Coast passive margin from large aperture seismic experiments (LASE), *Mar. Petrol. Geol.*, **3**, 234–242.

Lowrie, W., 1974. Oceanic basalt magnetic properties and the Vine and Matthews hypothesis, *Geophysics*, **40**, 513–536.

Lowrie, W., 1977. Intensity and direction of magnetisation in oceanic basalts, *J. Geol. Soc. Lond.*, **133**, 61–82.

Lowrie, W., 1979. Geomagnetic reversals and ocean crust magnetisation, in *Deep Drilling Results in the Atlantic Ocean Ocean Crust*, Maurice Ewing Series 2, pp. 135–150, eds Talwani, M., Harrison, C. G. & Hays, D. E., American Geophysical Union, Washington, DC.

Masson, D. G. & Miles, P. R., 1984. Mesozoic seafloor spreading between Iberia, Europe and North America, *Mar. Geol.*, **56**, 279–287.

Masson, D. G. & Miles, P. R., 1986. Structure and development of Porcupine Seabight sedimentary basin offshore southwest Ireland, *Am. Assoc. Petrol. Bull.*, **70**, 536–548.

Masson, D. G., Montadert, L. & Scrutton, R. A., 1984. Regional geology of the Goban Spur continental margin, in *Initial Reports Deep Sea Drilling Project, 80*, pp. 1115–1139, US Government Printing Office, Washington DC.

Mauffret, A. & Montadert, L., 1987. Rift tectonics on the passive continental margin off Galicia (Spain), *Mar. Petrol. Geol.*, **4**, 49–70.

Mauffret, A. & Mondadert, L., 1988. Seismic stratigraphy off Galicia, *Sci. Results, ODP 103*, pp. 13–30, US Government Printing Office, Washington, DC.

Mauffret, A., Mougenot, D., Miles, P. R. & Malod, J. A., 1990. Cenozoic deformation and Mesozoic abandoned spreading centre in the Tagus Abyssal Plain (West of Portugal). Results of a multichannel seismic survey, *Can. J. Earth Sci.*, **26**, 1101–1123.

Meador, K. J. & Austin, J. A. Jr, 1988. A seismic comparison of the early stratigraphic evolution of conjugate passive continental margins. The Newfoundland/Flemish Basin and the eastern Iberian Abyssal Plain south of Galicia Bank, *Sci. Results, ODP 103*, pp. 777–786, US Government Printing Office, Washington, DC.

Meador, K. J., Austin, J. A. & Dean, D. F., 1988. Shelf-to-basin correlation off eastern Canada: developing a seismic stratigraphic framework in the Northern Newfoundland basin, in *Atlas of Seismic Stratigraphy*, vol. 2, pp. 88–95, ed. Bally, A. W., AAPG Studies in Geology No. 27, Tulsa, OK.

Mendes-Victor, L. A., Hirn, A. & Veinante, J. L., 1980. A seismic section across the Tagus valley, Portugal: possible evolution of the crust, *Ann. Geophys.*, **36**, 469–476.

Montadert, L., Winnock, E., Deltiel, J. R. & Grau, G., 1974. Continental margins of Galicia, Portugal and Bay of Biscay, in *The Geology of Continental Margin*, pp. 323–342 eds Burk, C. A. & Drake, C. L., Springer Verlag, New York.

Moreira, V. S., Prodehl, C., Mueller, St. & Mendes, A. S., 1982. Crustal structure of western Portugal, *Proc. 17th Gen. Assoc. European Seismol Comm., Budapest, 1980*, Publ. House, Hungarian Acad. Sci., Budapest.

Morgan, G. E., 1979. Palaeomagnetic results from DSDP site 398, in *Initial Reports of the Deep Sea Drilling Project, 47*, part 2, pp. 599–611, US Government Printing Office, Washington, DC.

Morgan, W. J., 1981. Hotspot tracks and the opening of the Atlantic and Indian Oceans, in *The Sea*, vol. 7, pp. 443–487, ed. Emiliani, C., Wiley-Interscience, New York.

Mougenot, D., 1988. Geologie de la Marge Portugaise, *Thèse de Doctorat D'Etat és Sciences Naturelles*, Université Pierre et Marie Curie, Paris VI.

Mougenot, D., Monteiro, J. H., Dupeuple, P. A. & Malod, J., 1979. La marge continentale sud-portugaise; evolution structurale et sedimentaire, *Ciencias de Tierra*, **5**, 223–246.

Mougenot, D., Kidd, R. B., Mauffret, A., Regnauld, H., Rothwell, R. G. & Vanney, J. R., 1984. Geological interpretation of combined Sea Beam, GLORIA and seismic data from Porto and Vigo seamounts, Iberian continental margin, *Mar. geophys. Res.*, **6**, 329–353.

Ogg, J. G., 1988. Early Cretaceous and Tithonian magnetostratigraphy of the Galicia Margin (Ocean Drilling Program Leg 103), *Sci. Results, ODP 103*, pp. 659–684, US Government Printing Office, Washington, DC.

Olivet, J.-L., Bonnin, J., Beuzart, P. & Auzende, J.-M., 1984. Cinématique de l'Atlantique Nord et Central, *Rapports Sci. et Techniques*, **54**, CNEXO 108.

Peal, K. R. & Kirk, R. E., 1983. An event recording ocean bottom seismograph, *IEEE Proceedings of 3rd Working Symposium on Oceanographic Data Systems*, pp. 114–118, IEEE Computer Society, Silver Spring, MD.

Pitman, W. C. & Talwani, M., 1972. Sea floor spreading in the North Atlantic, *Bull. geol. Soc. Am.*, **83**, 619–649.

Rabinowitz, P. D., Cande, S. & Hayes, D. E., 1979. The J-Anomaly in the central N. Atlantic Ocean, in *Initial Reports of Deep Sea Drilling Project, 43*, pp. 879–885, US Government Printing Office, Washington, DC.

Regan, R. D. & Rodrigues, P., 1981. An overview of the external magnetic field with regard to magnetic surveys, *Geophys. Surv.*, **4**, 255–296.

Ryall, P. J., Hall, H. M., Clark, J. & Milligan, T., 1977. Magnetisation of oceanic crustal layer 2—results and thoughts after DSDP Leg 37, *Can. J. Earth Sci.*, **14**, 684–706.

Sibuet, J.-C., Ryan, W. B. F. & Shipboard Scientific Party, 1979. *Initial Reports Deep Sea Drilling Project, 47*, US Government Printing Office, Washington, DC.

Sibuet, J.-C., Maze, J.-P., Amortila, P. & Le Pichon, X., 1987. Physiography and structure of the western Iberian Continental margin off Galicia, from Seabeam and seismic data, *Initial Reports, ODP 103*, pp. 77–79, US Government Printing Office, Washington, DC.

Srivastava, S. P. & Tapscott, C. R., 1986. Plate kinematics of the North Atlantic, in *Geology of North America*, vol. M, chapter 3, pp. 379–404, eds Vogt, P. R. & Tucholke, B. E., Geol. Soc. Am., Boulder, CO.

Srivastava, S. P., Verhoef, J. & MacNab, R., 1988. Results from a detailed aeromagnetic survey across the northeast Newfoundland margin, Part II. Early opening of the North Atlantic between the British Isles and Newfoundland, *Mar. Petrol. Geol.*, **5**, 324–337.

Sullivan, K. D., 1983. The Newfoundland Basin: ocean–continent boundary and Mesozoic seafloor spreading history, *Earth planet. Sci. Lett.*, **2**, 321–339.

Talwani, M. & Eldholm, O., 1972. Continental margin off Norway: A geophysical study, *Geol. Soc. Am. Bull.*, **83**, 3575–3606.

Thommeret, M., Boillot, G. & Sibuet, J.-C., 1988. Structural map of the Galicia Margin, *Sci. Results, ODP 103*, pp. 31–36, US Government Printing Office, Washington, DC.

Tucholke, B. E. & Ludwig, W. J., 1982. Structure and origin of the J anomaly Ridge, western North Atlantic Ocean, *J. geophys. Res.*, **87**, 9389–9407.

Verhoef, J., Collette, B. J., Miles, P. R., Searle, R. C., Sibuet, J.-C. & Williams, C. A., 1986. Magnetic anomalies in the Northeast Atlantic Ocean (35°–50°N), *Mar. geophys. Res.*, **8,** 1–25.

Vogt, P. R., 1986. Magnetic anomalies and crustal magnetisation, in *Geology of North America,* vol. M, pp. 229–256, eds Vogt, P. R. & Tucholke, B. E., Geol. Soc. Am., Boulder, CO.

White, R. S. & McKenzie, D. P., 1989. Magnetism at rift zones: the generation of volcanic continental margins and flood basalts, *J. geophys. Res.*, **94,** 7685–7729.

White, R. S., Detrick, R. S., Sinha, M. C. & Cormier, M. H., 1984. Anomalous seismic crustal structure of oceanic fracture zones, *Geophys. J. R. astr. Soc.*, **79,** 779–798.

Whitmarsh, R. B., Avedik, F. & Saunders, M. R., 1986. The seismic structure of thinned continental crust in the northern Bay of Biscay, *Geophys. J. R. astr. Soc.*, **86,** 589–602.